Petroleum 11 (2025) 23–40

Contents lists available at ScienceDirect

Petroleum

journal homepage: www.keaipublishing.com/en/journals/petlm

Full Length Article

Untreatment reutilization of high-salinity flowback fluid and produced water to prepare fracturing fluid by using associative thickener

Yan Liang [a, *], Sukai Wang [a, **], Guiyi Zhang [b, ***], Yonglong Li [a], Wei Liu [a], Songlin Pu [a], Lipeng Zhang [a], Tianxiang Wang [a], Lianghui Wan [a], Xionghui Liu [a]

[a] Engineering Technology Research Institute, CNPC Western Drilling Engineering Co., LTD, Karamay, 834000, China
[b] Drilling Fluid Company, CNPC Western Drilling Engineering Co., LTD, Karamay, 834000, China

ARTICLE INFO

Article history:
Received 23 October 2024
Received in revised form
8 December 2024
Accepted 21 December 2024

Keywords:
Hydraulic fracturing
Flowback fluid
Produced water
Reutilization without treatment
Drag reduction and sand-carrying
Associative thickener
Physical and chemical interaction

ABSTRACT

Reutilizing flowback fluid and produced water to prepare fracturing fluid is still an urgent problem that needs to be solved and is not well solved. In this work, an anti-salt associative thickener (AAT) was synthesized by free radical copolymerization, and the molecular structure of AAT was demonstrated by FTIR and ^{1}H-NMR. Furthermore, compared with a common anti-salt thickener (HAT), the comprehensive performances of AAT were systematically investigated under the conditions of fresh water, flowback fluid and produced water in Sulige Gasfield. The results show that under the conditions of an average salinity of 34,428 mg/L and an average high-valent ion content of 4967 mg/L, AAT can present good thickening capacity, temperature and shear resistance, drag reduction efficiency, sand-carrying ability, gel-breaking property and high-effective crosslinking capacity with organic zirconium crosslinker at high salinity, which implicates the great potential and feasibility to prepare fracturing fluid by reutilizing high-salinity flowback fluid and produced water without further treatment. Moreover, the possible mechanisms of the associative thickener to achieve high-effective drag reduction and sand-carrying might be the existence of reversible supramolecular structures and the significant increase of viscoelasticity by shear stretching in turbulent state. At the same time, both physical and chemical interaction can make a significant contribution to high-effective crosslinking capacity of associative thickener. All results and findings can provide an important reference for the design of novel fracturing fluid and the reutilization of high-salinity water in stimulation applications.

1. Introduction

Reservoir stimulation is an important technical method to realize large-scale and cost-effective development of unconventional (tight, shale, coal seam etc.) or low/ultra-low permeability oil and gas resources [1–6]. Over past decades, as an key stimulation technology, hydraulic fracturing has been widely applied to reservoir stimulation and has made outstanding contributions to the stable energy supply and national strategic security all over the world, especially in China [7].

Sulige Gasfield is the largest onshore integrated tight sandstone gas reservoir in China, and the current gas production has exceeded 300×10^8 m^3/a [8]. Achieving the continuous large-scale development of Sulige Gasfield is of great significance to increase oil and gas resources in China. However, the gas field is characterized as low permeability, low pressure and low gas abundance, and the large-scale and cost-effective development of the field needs to rely on the hydraulic fracturing [8,9]. During hydraulic fracturing and gas production, a large number of high-salinity flowback fluid and produced water are continuously discharged from wellbore and produced to the surface, which brings a huge post-processing challenge for operators and oil-gas workers in view of the strict requirement of environmental protection. Because of the

* Corresponding author.
** Corresponding author.
*** Corresponding author.
E-mail addresses: gyfzly@126.com (Y. Liang), wangsukai@cnpc.com.cn (S. Wang), zhanggy@cnpc.com.cn (G. Zhang).
Peer review under the responsibility of Editorial Office of Petroleum.

https://doi.org/10.1016/j.petlm.2024.12.003

complicated components, high salinity, high metal ion content, high suspended solid content and high oil content, it is very difficult and expensive to achieve the external discharge flowback fluid and produced water after fine treatment [8,10–14]. Therefore, reutilizing flowback fluid and produced water to prepare the fracturing fluid has attracted growing attention, and has been regarded as one of the most economical and eco-friendly technical means [15].

It is well-known that fracturing fluid is a key chemical working fluid that should be used during hydraulic fracturing, and its comprehensive performances, including thickening capacity, resistance to high temperature and shear, drag reduction efficiency, etc., determine the final stimulation effect to a great degree [16–22]. However, during reusing flowback fluid and produced water, the hydration-swelling capacity and crosslinking property of thickeners can be remarkably weakened by high salinity, especially divalent and trivalent metal ions, etc., leading to the fracturing fluids formed by widely used guar gum or conventional polymer cannot meet the requirements well under the conditions of high salinity [23–28]. To weaken even avoid the aforementioned problems, many available literatures have been reported and different approaches have been pointed out [29–37]. In summary, the main solving ideas include two aspects: one is achieving the reuse of high-salinity water by removing high-valence ions and other unfavorable components through different water-treatment equipment and technologies or to mask metal ions by chelating agents; another is to develop the fracturing fluids with strong salt-resistance.

Liang et al. [38] proposed a cheap and effective method to reuse the flowback fluid to prepare the recycled guar gel by through filtering, decoloring and chelating. The results showed that the performance of recycled gel is similar to that of original gel or even better. Coomarasamy et al. [39] investigated the effect of produced water on the performances of guar-based fracturing fluid by a series of laboratory measurements and then demonstrated the feasibility of preparing fracturing fluid using produced water. Ke et al. [40] analyzed the main influencing factors on the performance of fracturing fluid prepared by flowback fluid in Sulige Gasfield, and the results showed that divalent ions (Ca^{2+}, Mg^{2+} and Fe^{2+}) have the greatest effect, which can be solved by simultaneously adding the chelating or precipitation agent and diluting with some fresh water. Yao et al. [25] reported a cost-effective method to prepare a guar fracturing fluid with high-salinity water through organophosphate chelating agent, which can obtain a final viscosity above 50 mPa·s after shearing for 80 min under 170 s^{-1} and 150°C. Mao et al. [41] prepared a concentrated suspension thickener with the copolymerization of acylamide, acrylic acid, 2-acrylamino-2-methylpropyl sulfonic acid and a double quaternary ammonium monomer, and the measurements showed that the thickener has excellent salt-resistance in high-salinity solutions and has the application potential in sewage treatment. All the literatures are not listed here, and the relating results and findings have indicated that it is possible to reuse flowback fluid or produced water relying on some methods or technologies. However, as the increasing demand of cost-effective development, it is an inevitable trend to realize the reutilization of flowback fluid or produced water without any treatment.

In this work, compared with the common anti-salt thickener, the comprehensive performances (involving thickening capacity, temperature and shear resistance, drag reduction efficiency, proppant-carrying ability and gel-breaking property, etc.) of an anti-salt associative thickener (AAT) and a crosslinking system composed of AAT with organic zirconium crosslinker were respectively investigated under the conditions of fresh water, flowback fluid and produced water in Sulige Gasfield. The results show that AAT can present good anti-salt performance and an excellent crosslinking capacity at high salinity, which implicate the great potential and feasibility of untreatment reutilization of high-salinity flowback fluid and produced water. At the same time, the possible mechanisms of associative thickener, including significant drag reduction, high-effective sand-carrying and crosslinking, were proposed to provide a reference for further understanding the relating mechanisms of some novel fracturing fluids.

2. Experimental section

2.1. Materials

Anti-salt associative thickener (AAT), which has a hydrolysis degree of 24.3 mol%, a viscosity-average molecular weight of 934×10^4 Da and an associative monomer content of 0.5 wt%, was prepared in laboratory by the copolymerization of acrylamide (AM), sodium acrylate (NaAA), 2-acrylamide-2-methylpropane sulfonate (AMPS) with a small amount of cetylmethyldiallyl ammonium chloride (C16MDAC), and the molecular structure of AAT is shown in Fig. 1; high anti-salt thickener without associative monomer (HAT), which has a hydrolysis degree of 25.2 mol%, a viscosity-average molecular weight of 1950×10^4 Da and a higher AMPS content, was also prepared in laboratory as the same method. The specific preparation process and characterization are given later. Industrial white oil was purchased from Northwest Lubricating Oil Branch of CNPC; AM, NaAA, AMPS, C16MDAC, sorbitan monostearate, polyoxyethylene sorbta monopalmitate, fatty alcohol polyoxyethylene ether, zirconium oxychloride, sodium lactate, oxalic acid, sodium hydroxide, sodium bicarbonate, sodium ethylene diamine tetraacetate, water-soluble azo initiator, potassium persulfate (KPS), ethyl alcohol and ammonium persulfate (APS) were purchased from Chengdu Kelong Chemical Reagent Factory; modified bentonite was purchased from Zhejiang Fenghong New Materials Co., LTD. Ceramsite proppant (40–70 or 30–40 mesh), different flowback fluids and produced water were provided by Sulige Gasfield Branch of CNPC Western Drilling Engineering Co., LTD, and the main ion components of flowback fluids and produced water were given later. Unless otherwise specified, the purity of all materials is chemical grade and the materials were not further treated before use.

2.2. Synthesis of thickeners

The thickeners were synthesized by free radical copolymerization in aqueous solution. A specific synthesis process of AAT was as follows. At a fixed monomer content of 25 wt%, the stoichiometric AM, NaAA, AMPS and C16MDAC were added into a beaker to homogenize by stirring at room temperature. And then the pH of resulting mixture was adjusted to be approximately 8 by a certain

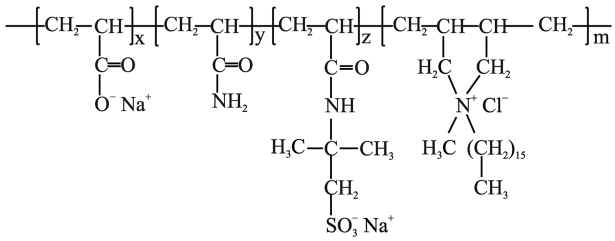

Fig. 1. Molecular structure of AAT.

amount of sodium bicarbonate and the mixture was placed into a freezer to reduce the temperature to be 0°C within 30 min. Afterwards, 2.5 mL of composite initiator of water-soluble azo initiator with potassium persulfate was added to initiate the polymerization reaction for 5 h, and the resulting colloid was adequately cooled to room temperature and cut into small pieces. Finally, the small pieces were repeatedly washed and precipitated in ethyl alcohol and were vacuum-dried for 5 h at 60°C to obtain AAT thickener powder. The HAT was also prepared as the same process.

2.3. Characterization of thickeners

Using the measurements involving Fourier-transform infrared (FTIR) spectroscopy and proton nuclear magnetic resonance (^{1}H-NMR), the thickeners were characterized qualitatively. FTIR spectra was obtained with the potassium bromide tablet method on a Nicolet 6700 FTIR spectrometer (Thermo Fisher), and ^{1}H-NMR measurements were conducted using heavy water as the solvent on a Bruker AV-III NMR spectrometer (400 MHz, Bruker BioSpin, Switzerland).

2.4. Preparation of organic zirconium crosslinker

The stoichiometric fresh water was added into a 250 mL three-necked flask and placed in a magnetic stirring thermostatic water bath, and 16 g of zirconium oxychloride was weighed and added into the three-necked flask to completely dissolve by stirring at 50°C. And then 18 g of oxalic acid and 9 g of sodium lactate was orderly added and homogenized within 30 min to form a milky-white mixture. Afterwards, a certain amount of sodium hydroxide aqueous solution (20 wt%) was used to adjust the pH value of resulting mixture to be approximately 7.5. Finally, a clear and transparent crosslinker liquid (namely GJL) was obtained after continuously reacting for 8 h. During the reaction, a condensing reflux device was used to prevent liquid evaporation.

2.5. Physico-chemical analysis of flowback fluids and produced water

Cationic/anionic components and pH of flowback fluids and produced water were respectively measured by a PHS-3E pH Meter (INESA, China), a dionex aquion (AQ) Ion Chromatograph (Thermo Scientific, USA) and ionic titration. During the measurements, pH was determined without other pre-treatments. Whereas, the flowback fluids and produced water need to be filtered with 0.2 μm qualitative filter paper and diluted to a certain concentration using deionized water before the measurements of ion components.

2.6. Preparation of the suspended-emulsion

To achieve the advantages of short construction period, no fluid waste, and good economic cost and environmental friendliness, the thickener usually need to be used in the form of suspended-emulsion during hydraulic fracturing [42]. In this case, the thickeners (AAT and HAT) were made into the suspended-emulsion before use as the same method in our previous literature [43]. Specifically, a certain amount of industrial white oil was weighed into a 500 mL beaker and stirred to form an obvious vortex at a speed of 400 ± 10 r/min, and then 10 g of sorbitan monostearate and 5 g of polyoxyethylene sorbta monopalmitate were orderly added and homogenized for 30 min. Afterwards, 7.5 g of modified bentonite and 6 g of fatty alcohol polyoxyethylene ether were successively added and continued to stir for other 30 min, which followed by adding 100 g of thickener within 30 s to stir for more than 30 min. Thus, a milky-white suspended-emulsion with 40% thickener content, good fluidity and moderate bulk viscosity can be obtained.

2.7. Preparation and viscosity measurement of thickener aqueous solution

At room temperature, a certain amount of fresh water was first weighed into a beaker and made a vortex with a stirring speed of approximately 400 r/min. And then stoichiometric suspended-emulsion was added within 2 s and mixed for 2 min to obtain a series of stock thickener aqueous solution with different concentrations. Afterwards, the viscosity stable value within 2 min was measured and recorded using a six-speed rotating viscometer (ZNN-D6) at a rotation speed of 100 r/min (corresponding to a shear rate of 170 s^{-1}).

2.8. Measurements of temperature-shear resistance

Approximately 60 g of stock thickener solution was added into the coaxial cylinder of RS 6000 rheometer (HAAK, Germany) to measure the shearing viscosity using PZ38 magnetic rotor under the conditions of 120°C and 170 s^{-1}. Thus, the changing curves of shearing viscosity with shearing time and the stable shearing viscosity were obtained to further analyze the temperature-shear resistance. During the whole measurement, the temperature was first raised from 30 to 120°C at a heating rate of 5 °C/min and the duration time including the heating process was 120 min.

2.9. Measurements of static sand-carrying performance

The static sand-carrying testing has been regarded as an important means to evaluate the proppant-carrying capacity of fracturing fluid. Specifically, fixing sand-liquid volume ratio as 20%, the stoichiometric thickener solution was adequately mixed with ceramsite proppants (20–40 mesh) using high-speed disperser, and the resulting mixture was rapidly transferred into a 100 mL plug measuring cylinder to record the sedimentation time and sedimentation height until no status change. Afterwards, the sedimentation velocity of the proppants can be calculated according to Eq. (1).

$$V_S = \frac{H_S}{t_S} \tag{1}$$

Where, H_S refers to the stable sedimentation height of the proppants, cm; t_S refers to the stable sedimentation time of the proppants, min; V_S refers to the sedimentation velocity, cm/min.

2.10. Measurements of gel-breaking property

The gel-breaking property of single thickener solution and crosslinking gel were evaluated according to the method in our previous literature, in which the viscosity, surface tension and residue content of the gel-breaking liquid were measured for further analysis [43].

2.11. Measurements of drag reduction performance

The drag reduction efficiency of fracturing fluid is a key factor that significantly determine the pumping pressure and construction displacement of the hydraulic fracturing, which can be obtained by calculating the friction pressure drop caused by the flowing of different fluids in the pipeline [25]. In this case, the frictional differential pressure of fresh water (or flowback fluid or

produced water) and thickener solution was respectively measured by a SLSY pipeline friction test system with a pipe diameter of 10 mm (Jiangsu Haian Petroleum Scientific Research Instrument Company, China), and the drag reduction efficiency was calculated according to Eq. (2). During the measurements, the pumping displacement was 42 L/min and the duration time was fixed as 10 min.

$$FR = \frac{\Delta P_W - \Delta P_A}{\Delta P_W} \times 100 \quad (2)$$

Where, ΔP_W refers to the frictional differential pressure generated by the water, MPa; ΔP_A refers to the frictional differential pressure generated by thickener solution, MPa; *FR* refers to the drag reduction efficiency, %.

2.12. Measurements of online-crosslinking performance of thickener with crosslinker

As the same preparation method as that of aforementioned thickener aqueous solution, the crosslinking system with a constant concentration of thickener and crosslinker was first formed by simultaneously mixing organic zirconium crosslinker with thickener. And then 60 g of resulting system was placed in a thermostatic water bath to gelation at 90°C, and the crosslinking time was recorded and gel appearance was observed to evaluate the online-crosslinking performance. On the other hand, another 60 g of resulting system was timely placed on the RS 6000 rheometer to measure the temperature-shear resistance by online-crosslinking at 120°C and 170 s^{-1}.

3. Results and discussion

3.1. Molecular structure characterization of thickeners

The molecular structure of thickeners was characterized by FTIR and ^{1}H-NMR spectrograms, and the results are given in Figs. 2 and 3, respectively. As shown in Fig. 2(a), the spectrogram of HAT presented the strong absorption peaks at approximately 3444 cm^{-1} and 1644 cm^{-1}, which can be respectively assigned to the stretching vibration of N—H and C═O bond in the $CONH_2$ group. At the same time, a moderate absorption peak existed at approximately 1103 cm^{-1} can be assigned to the stretching vibration of SO_3^- group. Similarly, as shown in Fig. 2(b), the spectrogram of AAT also presented similar absorption peaks at approximately 3422 cm^{-1}, 1654 cm^{-1} and 1106 cm^{-1}. More importantly, it can be seen that some absorption peaks appeared at 2928 cm^{-1} and 1305 cm^{-1}, which might respectively correspond to the stretching vibrations of C—H bond in CH_3 group and C—N bond of associative monomer. On the other hand, the characteristic peaks around 1.56 and 2.14 ppm can be vividly seen from Fig. 3(a), which can be assigned to the protons of $-CH_2-$ and $-CH_3$ on macromolecular main chains, respectively. And the peaks between 3.03 and 3.05 ppm can be assigned to the protons of $-CH_2-$ attached by $-SO_3^-$ on macromolecular side chains. As for the spectrogram of AAT shown in Fig. 3(b), the chemical shifts ascribed to the protons of $-NCH_3$ and $-NCH_2-$ in associative monomer appeared at 3.26 ppm and 2.69 ppm, and the chemical shifts in the range of 1.11~1.15 and 3.55~3.62 can be ascribed to the protons of $-CH_3$ and $-CH_2-$ in the alkyl chains of associative monomer. The results demonstrate that all monomers have been incorporated into the thickeners and the expected molecular structure has been achieved.

3.2. Ion compositions and pH of flowback fluids and produced water

Different flowback liquids and produced water were retrieved from S block and Z block of Sulige Cooperative Development Zone in Sulige Gasfield, and the main physicochemical parameters were analyzed and are shown in Table 1 and Fig. 4. The apparent color of different flowback fluids mainly presented faint yellow or brown yellow, and that of produced water presented deep yellow or deep red. And the pH values of different flowback fluids and produced water are basically in the neutral range. Specifically, the value of the flowback fluid ranges from 7.0 to 8.0, and that of the produced water is nearly constant at 7. More importantly, it can also be noted

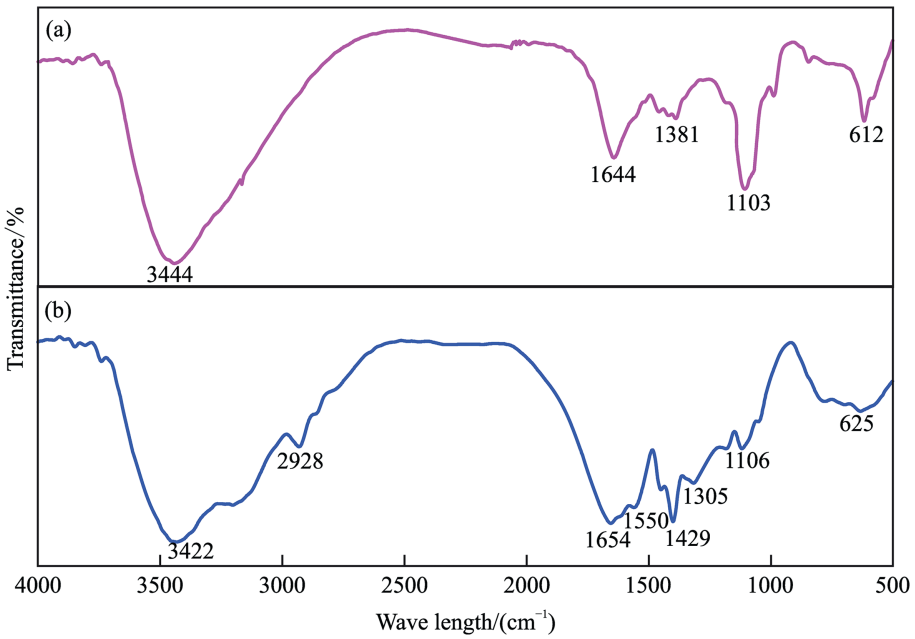

Fig. 2. FTIR spectrograms of HAT (a) and AAT (b).

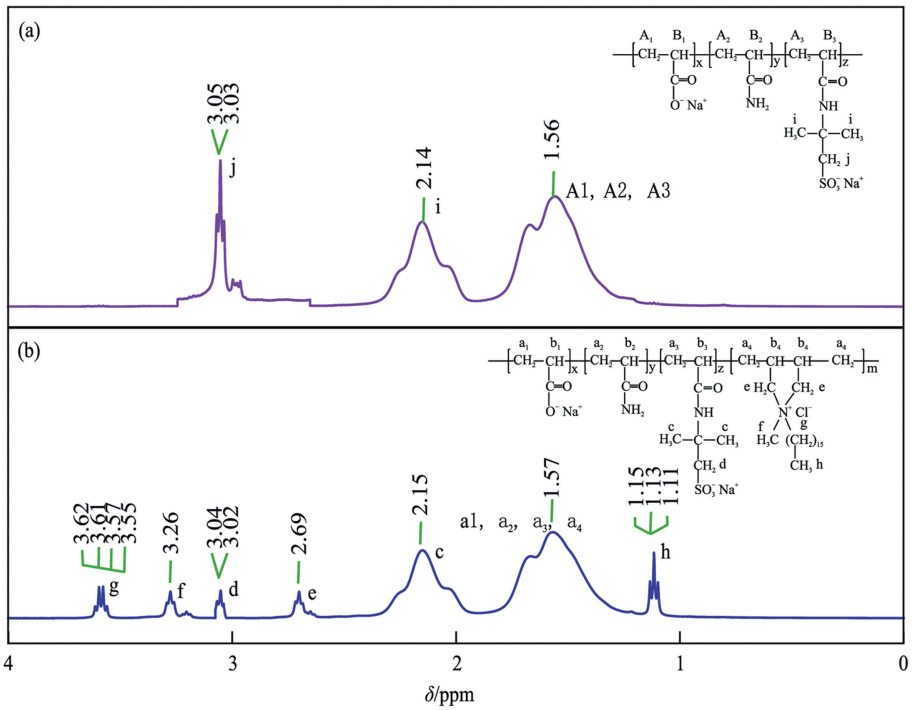

Fig. 3. ^{1}H-NMR spectrograms of HAT (a) and AAT (b).

Table 1
Apparent color, pH and ion components of different flowback fluids and produced water in S and Z blocks.

Water type	Well or Station No.	Apparent color	pH	Main ion content (mg/L)					
				Na^+	K^+	Ca^{2+}	Mg^{2+}	Cl^-	TDS
Flowback fluid	S-XX-17	Faint yellow	7.4	6913	7058	6854	576	23,093	45,000
	S-XX-2	Brown yellow	7.0	2378	4357	4018	446	18,654	30,400
	S-XX-23	Faint yellow	8.0	4236	4574	4162	461	18,804	33,000
	S-XX-14	Brown yellow	7.5	4321	6754	6691	384	23,093	42,000
	Z-XX-20	Faint yellow	8.0	3540	5583	5671	197	24,850	39,953
	Z-XX-32	Brown yellow	7.5	3018	2700	4831	193	18,815	29,565
Produced water	S-1#	Deep red	7.0	4492	1709	2803	239	18,460	27,786
	Z-1#	Deep yellow	7.0	4277	1529	3220	252	21,087	30,807
	Z-2#	Deep yellow	7.0	4155	3441	4499	256	27,406	40,323
	Z-3#	Deep red	7.0	3190	1798	3696	224	16,117	25,441
Average value			7.3	4052	3950	4645	323	21,038	34,428

that there are obvious differences among the ion contents of different flowback fluids or produced water, especially calcium and magnesium ions. That is, in all flowback fluids, that of S-XX-17 well has the highest monovalent and divalent ion content as well as total salinity, and that of Z-XX-32 well owns the smallest ion content and salinity. In all produced water, that of Z-2# Station and Z-3# Station has the highest and smallest ion content and salinity, respectively. By contrast, the ion content and salinity of flowback fluids are generally higher than that of produced water. Therefore, typically, the flowback fluids in S-XX-17 and Z-XX-32 wells and the produced water in Z-2# and Z-3# Stations (the appearance is shown in Fig. 5) were chosen to conduct the following researches.

3.3. Comprehensive performances of thickeners

3.3.1. Thickening capacity of thickeners

The viscosity of HAT and AAT as a function of the dosage of suspended-emulsion in a range of 0.1~2.5wt% was measured to investigate the thickening capacity of thickeners, and the results are plotted in Fig. 6. It can be seen that the viscosity increased with increasing dosage of suspended-emulsion and the variation is consistent with the concentration dependence of conventional water-soluble macromolecular polymers [44]. Moreover, it can also be noted that the viscosity of HAT nearly presented a linear variation with increasing dosage, but that of AAT first presented a slight increase at a lower dosage than 0.3 wt% or 0.4 wt% and then rapidly increased once the dosage beyond the aforementioned critical value. This is a unique characteristic of associative polymer and the critical value is usually called as critical association concentration (CAC), which is closely related to the associative effect between hydrophobic groups in macromolecular chains of associative polymer [44–46].

In addition, it can also be seen that AAT presented a higher viscosity than HAT both under the conditions of fresh water and different flowback fluids or produced water. That is, although the molecular weight of HAT is nearly twice that of AAT, AAT has noticeable thickening capacity than HAT even under the harsh conditions of high salinity and divalent ions. The results can be ascribed to that the thickening capacity of associative polymer was determined by molecular weight and the association effect

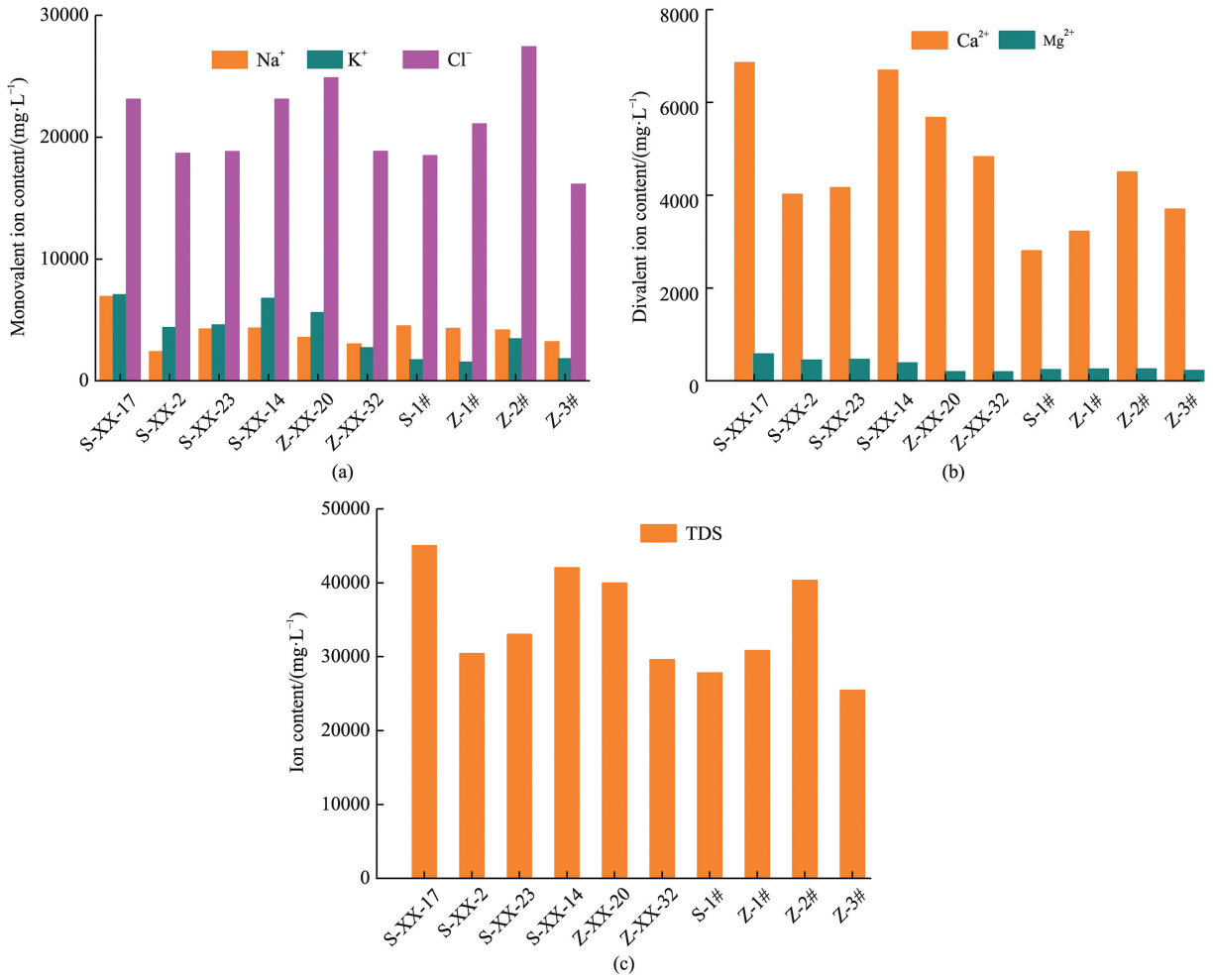

Fig. 4. Ion content of different flowback fluids and produced water in S and Z blocks: (a) monovalent ion; (b) divalent ion; (c) TDS.

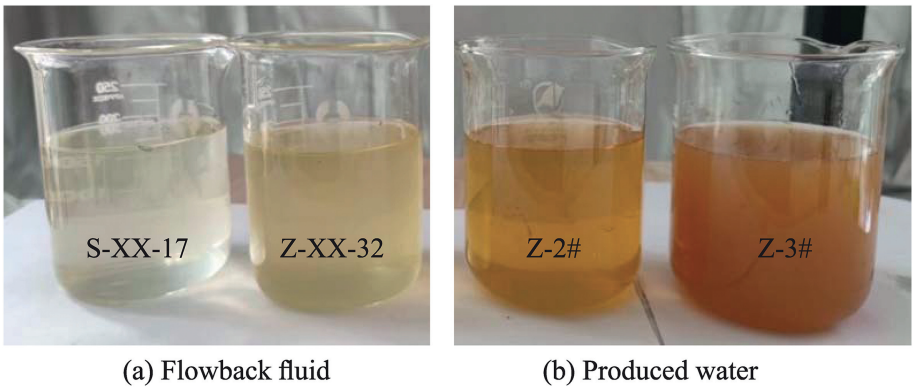

Fig. 5. Appearance of different flowback fluids (a) and produced water (b) in S and Z blocks.

between hydrophobic groups simultaneously [47]. High salinity, especially high divalent ions, can make the polymer chains become curly by electrostatic effect and reduced the hydromechanical size of the molecular chain, but the association interaction can also be remarkedly enhanced due to the increased polarity of the solution [48,49].

3.3.2. Temperature-shear resistance of thickeners

The temperature-shear resistance of fracturing fluid under the conditions of target reservoir is one of important performances to evaluate proppant-carrying capacity, and a stable shearing viscosity of not less than 50 mPa·s is generally required for achieving a good proppant-carrying using synthetic polymer-based fracturing fluid

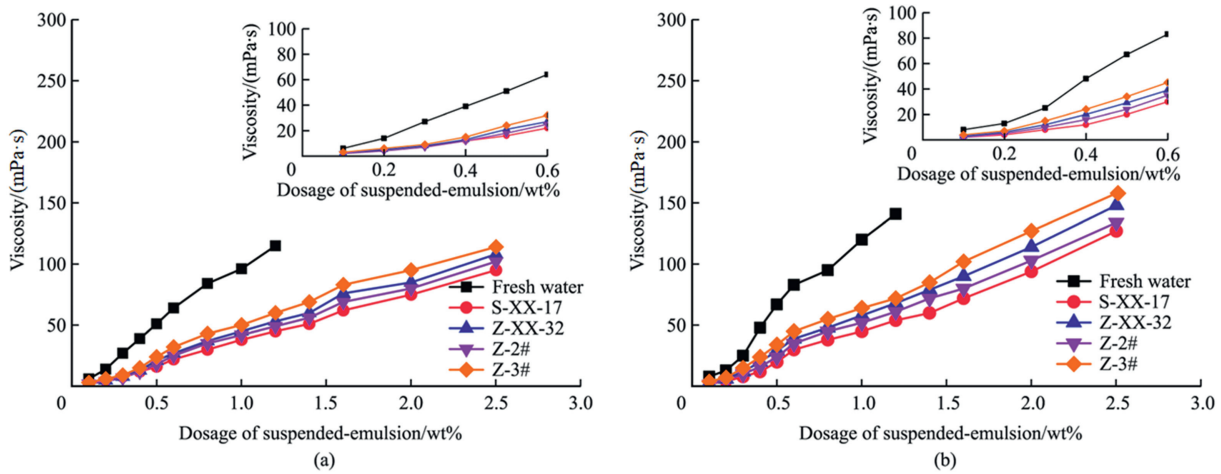

Fig. 6. Variation curves of the viscosity at different dosages of suspended-emulsion of HAT (a) and AAT (b).

at the stage of high sand ratio. The shearing viscosity of HAT and AAT within a shearing time of 120 min at different suspended-emulsion dosages of 0.5~0.9 wt% (for fresh water) and 1.0~2.5 wt% (for flowback fluid and produced water) was measured to investigate the temperature-shear resistance of thickeners, and the results are plotted in Figs. 7 and 8. It can be seen that the stable shearing viscosity gradually increased with increasing dosage, but there was obvious difference compared AAT with HAT. Specifically, AAT presented the similar variation trend with HAT in fresh water, and a stable shearing viscosity of larger than 50 mPa·s was achieved once the dosage was increased to 0.9 wt%. Moreover, AAT can achieve a shearing viscosity above 50 mPa·s at a dosage of 2.0 wt% or higher in different flowback fluids and produced water. However, as for HAT, the shearing viscosity was generally less than 50 mPa·s even if the dosage was increased to 2.5 wt%. The results indicate that AAT has better temperature-shear resistance than HAT in different high salinity brines. And the main reasons can be ascribed to two aspects: one is that the lower molecular weight of AAT is more benefit to shear resistance; another is that the associative interaction can further enhance the resistance to high temperature and high salinity.

In addition, the temperature-shear measurements of 2.5 wt% AAT under different ratios of S-XX-17 flowback fluid or Z-2# produced water to fresh water were also conducted to investigate the effect of dilution ratio on temperature-shear resistance, and the results are shown in Fig. 9. It can be seen that when the proportion of fresh water was gradually increased from 1:1 to 1:3, the final stable shearing viscosity of AAT only presented a slight increase compared with that without dilution, which indicates that the dilution using fresh water has no significant effect on temperature-shear resistance in the dilution ratio concerned. Therefore, it can be concluded that using AAT as the thickener can meet the technical requirement of temperature-shear resistance to reutilize the flowback fluid or produced water without further treatment.

3.3.3. *Static sand-carrying capacity of thickeners*

The static sand-carrying capacity of fracturing fluid is also one of important performances to evaluate proppant-carrying capacity, and the stronger the static sand-carrying capacity generally implies the better proppant-carrying effect. The static sand-carrying measurements of thickeners were conducted under different conditions and the results are shown in Table 2 and Fig. 10. It can be seen from that the total settling time of proppant increased but the settling rate of proppant decreased when the viscosity was gradually increased from 10 mPa·s to 45 mPa·s or 95 mPa·s. Furthermore, the settling rate of proppant at fresh water was significantly smaller

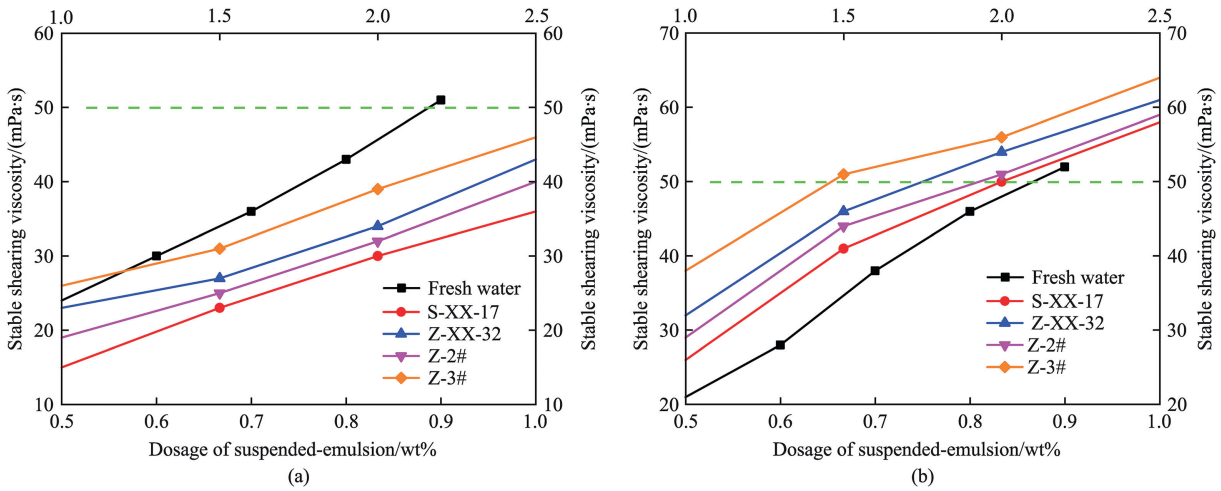

Fig. 7. Variation curves of stable shearing viscosity at different dosages of suspended-emulsion of HAT (a) and AAT (b).

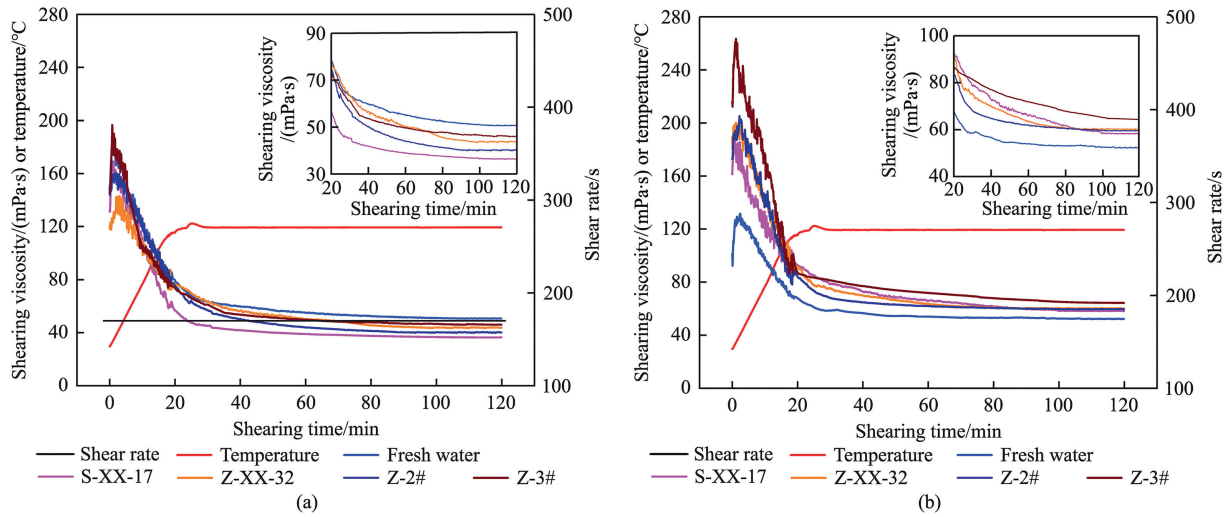

Fig. 8. Variation curves of shearing viscosity as a function of shearing time at a fixed dosage (0.9 wt% or 2.5 wt%) of suspended-emulsion of HAT (a) and AAT (b).

than that under the conditions of flowback fluid and produced water, which indicates that the static sand-carrying capacity of thickeners can be noticeably weakened by metal ions (especially high-valent ions) even at the same viscosity. More importantly, as shown in Fig. 10, AAT presented a smaller settling rate than HAT at the same viscosity, which can also be vividly demonstrated from the images shown in Fig. 11. That is, AAT has a better static sand-carrying performance than HAT at the same viscosity, and the specific mechanism was discussed later.

3.3.4. Gel-breaking property of thickeners

The gel-breaking property of fracturing fluid is a very important performance to evaluate reservoir damage and flowback capacity, and a viscosity of not exceeding 5 mPa·s, a surface tension of not exceeding 28 mN/m and a residue content of not exceeding 50 mg/L are generally required for the gel-breaking fluid to achieve a good flowback effect using synthetic polymer-based and non-gelled fracturing fluid after fracturing construction [50]. The gel-breaking property of thickeners were measured at a fixing thickener dosage of 2.5 wt% and in a dosage range of gel-breaker (namely APS) from 0.03 wt% to 0.04 wt%, and the results are shown in Table 3. It can be seen that the thickeners can be completely gel-broken after 90 min when APS dosage was increased to 0.035 wt%, namely the viscosity, surface tension and residue content of the gel-breaking liquid are very small. When APS dosage was further increased to 0.04 wt%, the gel-breaking effect was not improved obviously. More importantly, AAT can also present a good gel-breaking effect under the conditions of flowback fluid and produced water at a larger dosage than 0.03 wt%, indicating that AAT has hardly formation damage and it is easy to flowback after hydraulic fracturing.

3.3.5. Drag reduction performance of thickeners

The drag reduction performance of fracturing fluid is an important factor affecting construction pressure and displacement rate of hydraulic fracturing, and the higher drag reduction efficiency implies the lower construction pressure and the greater displacement rate. The drag reduction measurements of thickeners were conducted at a constant viscosity of 10 mPa·s and 20 mPa·s, and the results are shown in Table 4, Figs. 12 and 13. It can be seen

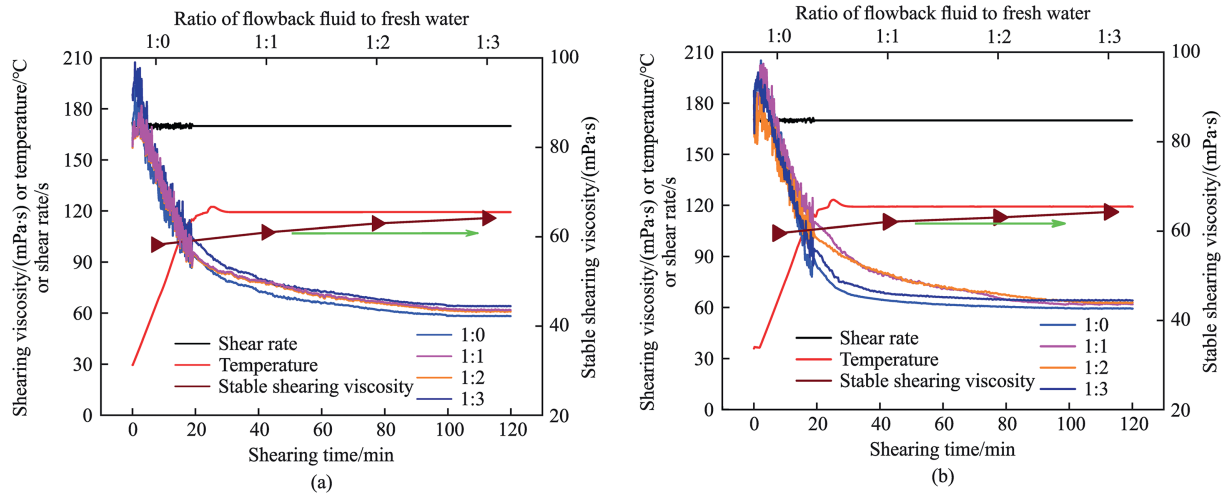

Fig. 9. Variation curves of shearing viscosity of 2.5 wt% AAT as a function of shearing time at different dilution ratios: (a) S-XX-17 flowback fluid; (b) Z-2# produced water.

Table 2
Static sand-carrying results of thickeners under different conditions.

Viscosity (mPa·s)	Thickener	Fresh water			Flowback fluid of S-XX-17			Produced water of Z-2#		
		Dosage (wt%)	Total settling time of proppant (min)	Settling rate of proppant (cm/min)	Dosage (wt%)	Total settling time of proppant (min)	Settling rate of proppant (cm/min)	Dosage (wt%)	Total settling time of proppant (min)	Settling rate of proppant (cm/min)
10	HAT	0.14	1.93	4.66	0.36	1.68	5.36	0.32	1.78	5.06
	AAT	0.15	1.89	4.76	0.35	1.75	5.14	0.25	1.83	4.92
45	HAT	0.46	17.5	0.51	1.2	12.3	0.73	0.9	14.7	0.61
	AAT	0.39	20.5	0.44	1.0	14.5	0.62	0.6	16.2	0.56
95	HAT	1.0	45	0.20	2.5	25	0.36	2.0	30	0.30
	AAT	0.8	60	0.15	2.0	35	0.26	1.5	39	0.23

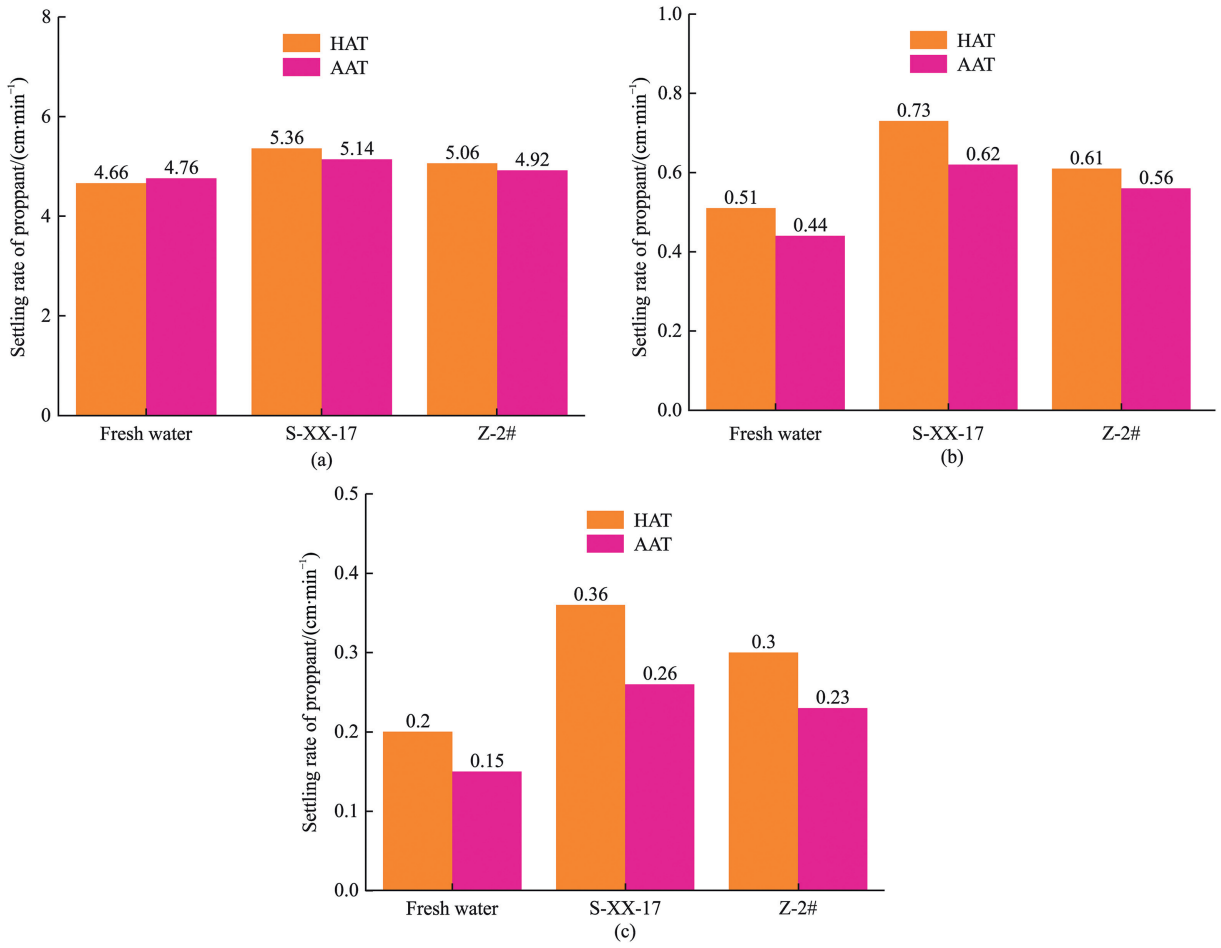

Fig. 10. Settling rate of proppant at different viscosities of thickener: (a) 10 mPa·s; (b) 45 mPa·s; (c) 95 mPa·s

that the average drag reduction efficiency decreased when the viscosity increased from 10 mPa·s to 20 mPa·s or the fracturing fluid was prepared by changing the fresh water to flowback fluid or produced water, but the drag reduction efficiency was greater than 70% in most cases. However, compared with HAT, AAT has always kept a higher drag reduction efficiency of above 72.41% and it was more than 3% higher than that of HAT under different conditions, indicating that AAT not only has a better static sand-carrying performance than HAT, but also can present a better drag reduction capacity than HAT at the same viscosity. This phenomenon can be mainly attributed to the significant drag reduction ability stemming from both the viscidity and elasticity of associative thickener. The specific mechanism was discussed later.

3.3.6. Possible mechanism of drag reduction and sand-carrying of associative thickener

Generally speaking, the key to achieve efficient drag reduction is to restrain the lateral flow and absorb the energy loss in turbulent state of fluids [51–53]. As shown in Fig. 14(a), due to the anti-salt thickener is a linear polymer, it has a smaller hydrodynamic size of molecular chains than the molecular aggregates of associative thickener, which cause the prevailing viscidity and weak elasticity, so that the drag reduction only depends on the distribution and entanglement of molecular chains along the flow lines to restrain the lateral flow. Moreover, the sand-carrying capacity mainly depends on the prevailing viscidity and limited elasticity for linear polymer.

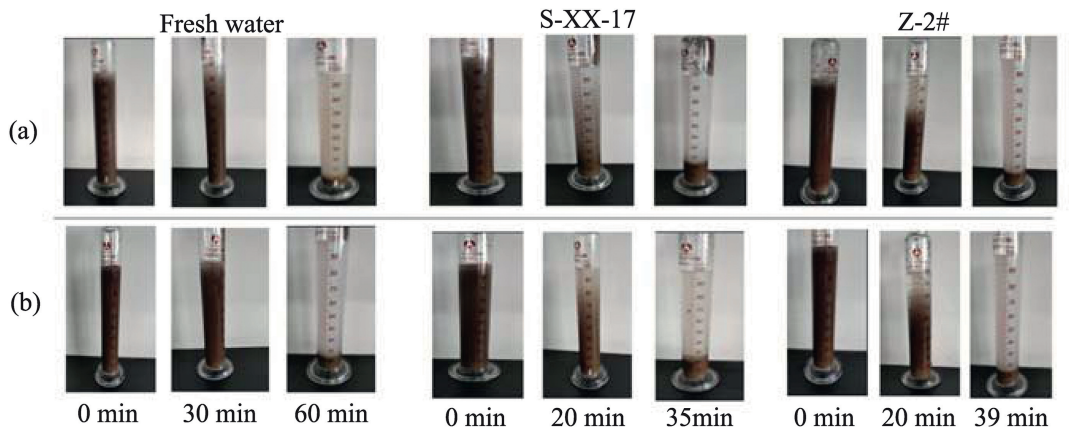

Fig. 11. Images of static sand-carrying measurements of thickener at a viscosity of 95 mPa·s: (a) HAT; (b) AAT.

Table 3
Gel-breaking property of 2.5 wt% thickener at different dosages of gel-breaker after gel-breaking for 90 min.

APS (wt%)	Thickener	Fresh water			Flowback fluid of S-XX-17			Produced water of Z-2#		
		Viscosity (mPa·s)	Surface tension (mN/m)	Residue content (mg/L)	Viscosity (mPa·s)	Surface tension (mN/m)	Residue content (mg/L)	Viscosity (mPa·s)	Surface tension (mN/m)	Residue content (mg/L)
0.03	HAT	4.75	27.15	36	4.45	27.04	48	4.45	27.35	45
	AAT	5.08	27.93	48	6.29	28.35	61	5.68	28.17	54
0.035	HAT	4.14	27.02	34	4.26	27.16	45	4.52	27.26	42
	AAT	4.56	27.41	42	4.82	27.82	48	4.73	27.73	46
0.04	HAT	4.02	27.12	38	4.12	27.04	44	4.11	27.24	43
	AAT	4.48	27.38	43	4.82	27.74	47	4.74	27.65	45

Table 4
Drag reduction results of thickeners under different conditions.

Viscosity (mPa·s)	Thickener	Fresh water		Flowback fluid of S-XX-17		Produced water of Z-2#	
		Dosage (wt%)	Average drag reduction efficiency (%)	Dosage (wt%)	Average drag reduction efficiency (%)	Dosage (wt%)	Average drag reduction efficiency (%)
10	HAT	0.14	73.58	0.36	70.43	0.32	71.31
	AAT	0.15	76.58	0.35	74.75	0.25	75.93
20	HAT	0.25	70.18	0.54	68.93	0.53	69.58
	AAT	0.25	74.39	0.5	72.41	0.45	72.89

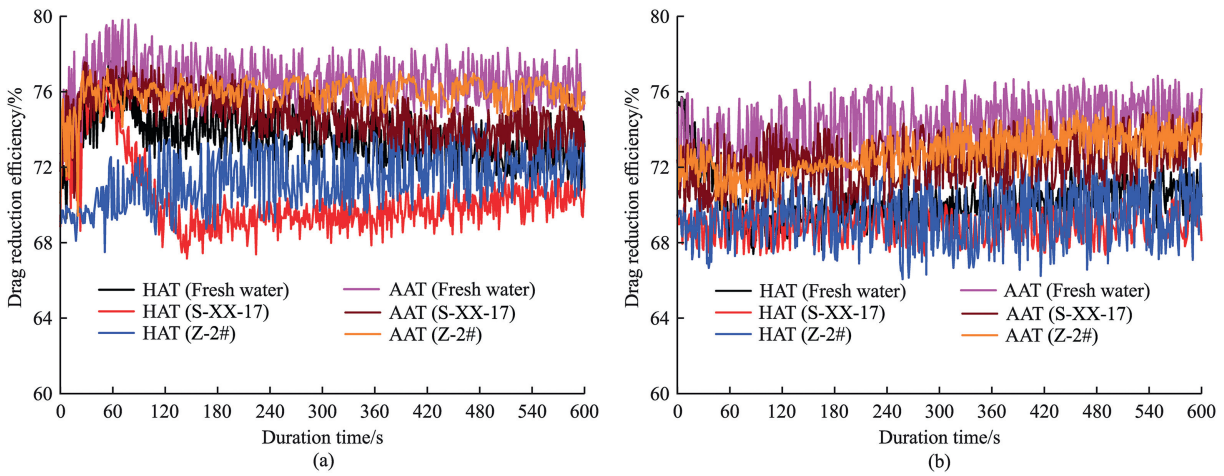

Fig. 12. Variation curves of drag reduction efficiency of thickeners as a function of duration time at a constant viscosity: (a) 10 mPa·s; (b) 20 mPa·s

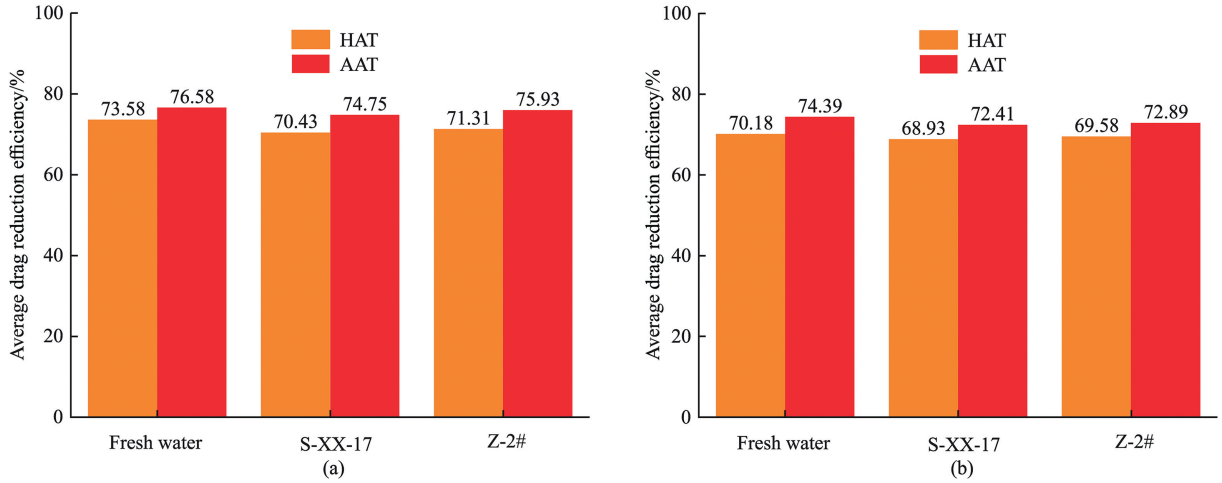

Fig. 13. Average drag reduction efficiency of thickeners at a constant viscosity: (a) 10 mPa·s; (b) 20 mPa·s

However, because of the existence of association effect in aqueous solution, the associative thickener can achieve high-effective drag reduction and sand-carrying through the possible two aspects shown in Fig. 14(b). On the one hand, the intramolecular association from associative thickener was untangled by strong shear stretching, so that the hydrodynamic size of the molecular chain increased and made it distribute along the flow lines, which restrain the lateral flow and reduce the friction. At the same time, the intramolecular association can be induced and transformed into the intermolecular association by higher shear, leading to the elasticity was obviously enhanced and the energy loss in turbulent state can be absorbed to improve the drag reduction efficiency. On the other hand, the stretching of intramolecular association and the transformation into the intermolecular association can significantly increase the hydromechanical size of molecular chains and enhance the viscoelasticity to some extent, which can achieve the sand-carrying through the combination of viscidity and elasticity. In other words, the associative thickener can meet the requirement of both high drag reduction and strong sand-carrying through the possible and reversible change of supramolecular structure in turbulent state.

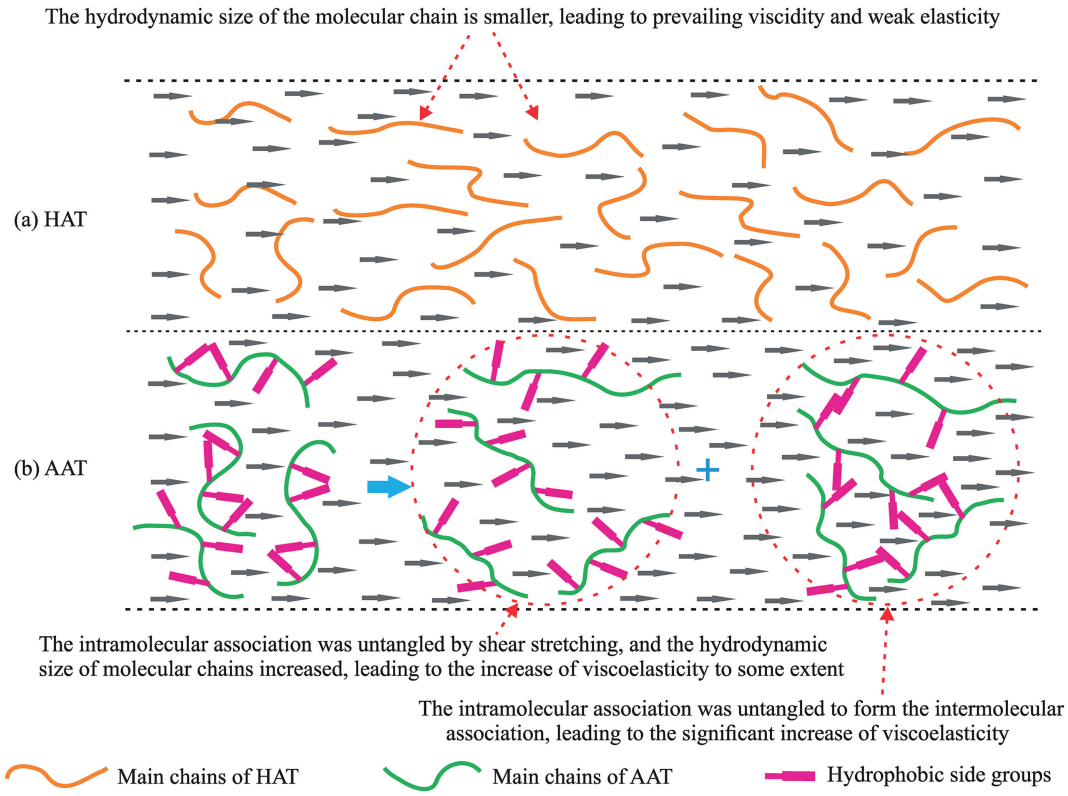

Fig. 14. Possible mechanism of drag reduction and sand-carrying of different thickeners.

3.4. Comprehensive performances of crosslinking system

3.4.1. Online-crosslinking performance of thickeners with crosslinker

During fracturing construction, online-crosslinking performance of fracturing fluid is a key factor to determine the construction security and final stimulation effect. To truly simulate the field construction, the thickeners was simultaneously mixed with crosslinker (GJL) to obtain the mixture, and a part of the resulting mixture was heated at 90°C to measure the crosslinking time and observe the gelation state. As shown in Table 5, under the condition of fresh water, the crosslinking performances of thickeners with crosslinker presented an overall changing trend of first increasing and then decreasing with increasing dosage of crosslinker, namely achieving the maximum crosslinking intensity corresponds to an optimal range of crosslinker. Moreover, as increased the dosage of suspended-emulsion to 0.6% or greater, the crosslinking performances can be further improved and the gelation state of 'complete crosslinking and strong hanging' can be obtained in a wider range of crosslinker. Compared with AAT, HAT can only achieve the gelation state of 'complete crosslinking and moderate hanging' at a suspended-emulsion dosage of 0.5% in the concerned range of crosslinker, and the gelation state of 'complete crosslinking and strong hanging' can only be obtained at a crosslinker dosage of 0.5% when the suspended-emulsion dosage was fixed as 0.6%, which can also be vividly seen from Fig. 15(a). However, even at a lower emulsion dosage of 0.5%, AAT can present the gelation state of 'complete crosslinking and strong hanging' in the crosslinker range of 0.3~0.4%, and the range can be further broaden to 0.3~0.5% (shown in Fig. 15(b)) and 0.2~0.6% at a emulsion dosage of 0.6% and 0.7%, respectively.

As shown in Table 6, under the conditions of flowback fluid and produced water, the changing trend of crosslinking performances with the increasing dosage of suspended-emulsion and crosslinker was similar to that under the condition of fresh water. However, it can also be seen that it was difficult for HAT to achieve the gelation state of 'complete crosslinking and general hanging' at an emulsion dosage of 1.0% in concerned crosslinker range and to achieve the gelation state of 'complete crosslinking and strong hanging' at an emulsion dosage of 1.2~1.4% in a wider crosslinker range (shown in Fig. 15(c)), which indicates that the crosslinking capacity of HAT has significantly deteriorated because of the presence of high-valent ions in flowback fluid and produced water. Fortunately, AAT can obtain the gelation state of 'complete crosslinking and strong hanging' in concerned emulsion dosage range of 1.0~1.4% and the applicable dosage range of crosslinker can broaden from 0.3% to 0.4%—0.3%~0.5%, which can also be vividly shown in Fig. 15(d). The results indicate that the AAT still has good crosslinking performance even under the harsh conditions and might be applied to a wide range of flowback fluid and produced water.

3.4.2. Temperature-shear resistance of crosslinking system through online-crosslinking

As mentioned above, HAT can crosslink with crosslinker (GJL) to achieve the gelation state of 'complete crosslinking and strong hanging' at an emulsion dosage of 1.2~1.4% and a crosslinker dosage of 0.5%, while AAT can obtain the same state in wider emulsion and crosslinker dosage range of 1.0~1.4% and 0.3~0.5%, respectively.

Table 5
Crosslinking results of thickeners with crosslinker in fresh water at 90 °C.

Thickener	Dosage of suspended-emulsion (wt%)	Dosage of crosslinker (wt%)	Crosslinking time (s)	Crosslinking performance
HAT	0.5	0.2	44~58	Weak crosslinking and almost no hanging
		0.3	45~72	Incomplete crosslinking and weak hanging
		0.4	45~84	Incomplete crosslinking and weak hanging
		0.5	45~112	Complete crosslinking and moderate hanging
		0.6	36~79	Incomplete crosslinking and weak hanging
		0.7	34~63	Incomplete crosslinking and weak hanging
AAT		0.2	40~117	Complete crosslinking and moderate hanging
		0.3	47~149	Complete crosslinking and strong hanging
		0.4	50~138	Complete crosslinking and strong hanging
		0.5	45~125	Complete crosslinking and moderate hanging
		0.6	40~105	Complete crosslinking and general hanging
		0.7	39~82	Incomplete crosslinking and weak hanging
HAT	0.6	0.2	43~60	Weak crosslinking and almost no hanging
		0.3	44~76	Incomplete crosslinking and weak hanging
		0.4	42~129	Complete crosslinking and moderate hanging
		0.5	45~136	Complete crosslinking and strong hanging
		0.6	43~121	Complete crosslinking and moderate hanging
		0.7	38~78	Incomplete crosslinking and weak hanging
AAT		0.2	42~121	Complete crosslinking and moderate hanging
		0.3	45~162	Complete crosslinking and strong hanging
		0.4	48~173	Complete crosslinking and strong hanging
		0.5	46~154	Complete crosslinking and strong hanging
		0.6	43~132	Complete crosslinking and moderate hanging
		0.7	40~101	Complete crosslinking and general hanging
HAT	0.7	0.2	41~80	Incomplete crosslinking and weak hanging
		0.3	45~119	Complete crosslinking and moderate hanging
		0.4	44~154	Complete crosslinking and strong hanging
		0.5	45~167	Complete crosslinking and strong hanging
		0.6	44~141	Complete crosslinking and strong hanging
		0.7	41~123	Incomplete crosslinking and weak hanging
AAT		0.2	46~176	Complete crosslinking and strong hanging
		0.3	44~182	Complete crosslinking and strong hanging
		0.4	50~201	Complete crosslinking and strong hanging
		0.5	48~192	Complete crosslinking and strong hanging
		0.6	45~175	Complete crosslinking and strong hanging
		0.7	44~121	Complete crosslinking and moderate hanging

Note: Crosslinking time is defined as the time between initial crosslinking and the largest crosslinking intensity, and the following is the same.

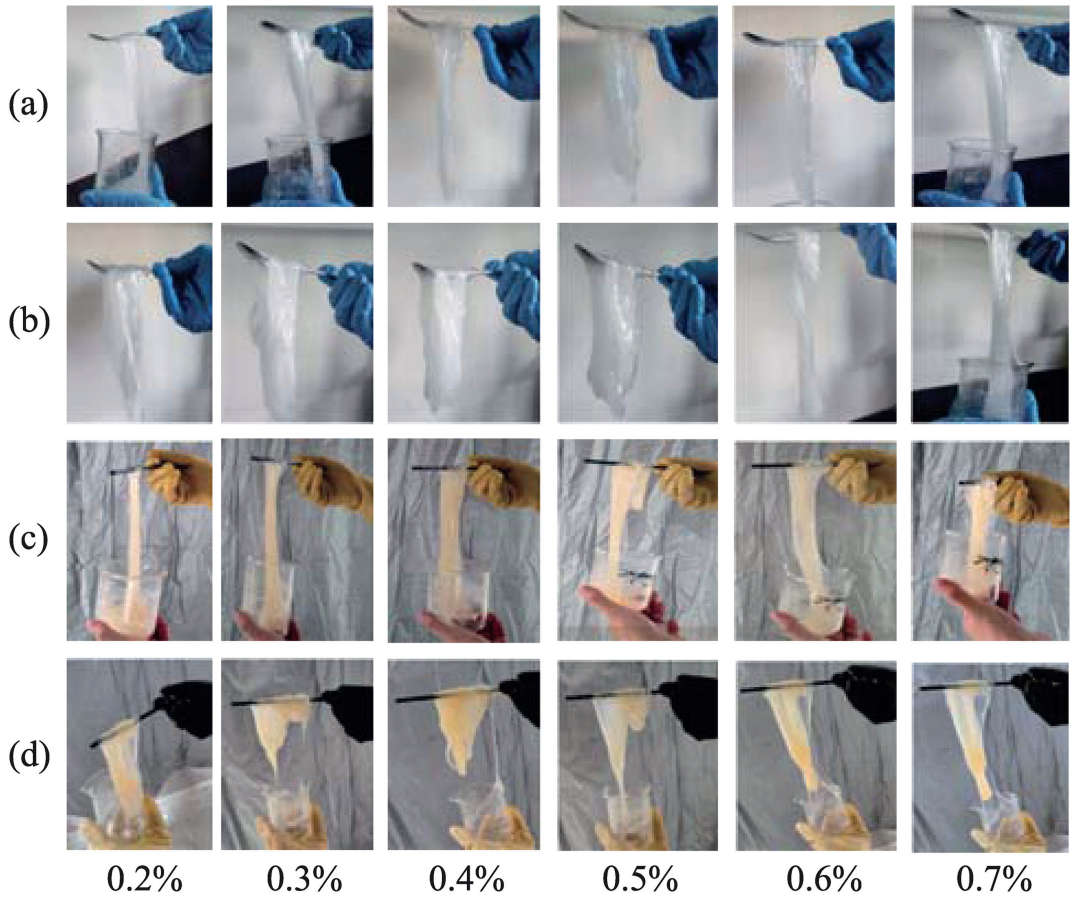

Fig. 15. Gelation state formed by the thickeners with crosslinker under different conditions at 90 °C: (a) 0.6% suspended-emulsion of HAT in fresh water; (b) 0.6% suspended-emulsion of AAT in fresh water; (c) 1.2% suspended-emulsion of HAT in Z-2# produced water; (d) 1.2% suspended-emulsion of AAT in Z-2# produced water.

Therefore, different mixture systems formed by simultaneously mixing thickener with crosslinker was placed on rheometer to measure the online-crosslinking behavior and to investigate the temperature-shear resistance, the results are shown in Fig. 16 and Table 7.

It can be seen that, under dynamic conditions of elevating temperature and continuous shear, different systems can achieve the crosslinking to a certain extent at a lower temperature and smaller time, and time and temperature range corresponding to maximum viscosity increased with increasing emulsion dosage. However, the system composed of HAT and GJL presented a relatively larger initial crosslinking time and temperature, and a lower stable shearing viscosity than 44 mPa s even the emulsion dosage was increased to 1.4%. On the contrary, the system formed by AAT and GJL exhibited a relatively smaller initial crosslinking time and temperature, and a greater stable shearing viscosity than 61 mPa·s in emulsion dosage range of 1.0~1.4%. The results indicate that the AAT not only has good online-crosslinking performance under the harsh conditions, but also owns excellent temperature-shear resistance, which can easily meet the general requirement of a stable shearing viscosity of not less than 50 mPa·s for synthetic polymer-based fracturing fluid at the stage of high sand ratio.

3.4.3. Static sand-carrying capacity of crosslinking system

The crosslinking systems with different gelation states in flowback fluid of S-XX-17 and produced water of Z-2# were used to conduct the static sand-carrying measurements, and the settling results and images of proppant are shown in Table 8 and Fig. 17, respectively. It can be seen from that the total settling time of proppant increased but the settling rate decreased when the emulsion dosage was increased from 1.2% to 1.4%, which can be ascribed to the enhanced gelation state shown in Table 8. More importantly, the settling rate of proppant for the crosslinking system formed by AAT was significantly smaller than that of HAT, which can also be vividly demonstrated from the images shown in Fig. 17. That is, AAT system has better static sand-carrying capacity than HAT system under the harsh conditions.

3.4.4. Gel-breaking property of crosslinking system

The gel-breaking property of the resulting gels formed by different crosslinking systems (namely 1.2% HAT+0.5% GJL and 1.2% AAT+0.3% GJL) were measured in a dosage range of gel-breaker (APS) from 0.03 wt% to 0.07 wt%, and the results are shown in Table 9. It can be seen that the gels cannot be completely gel-broken after 90 min when APS dosage was 0.03%, and the viscosity, surface tension and residue content of the gel-breaking liquid were relatively higher. Whereas, as increasing APS dosage to 0.05% or greater, the gel-breaking effect was significantly improved, and the viscosity, surface tension and residue content can meet the general requirements. In generally, the gel formed by AAT can also present a good gel-breaking effect under the conditions of flowback fluid and produced water at a larger dosage than 0.05%, and the characteristics of easy gel-breaking and low formation damage is noticeable.

Table 6
Crosslinking results of thickeners with crosslinker in flowback fluid and produced water at 90 °C.

Thickener	Dosage of suspended-emulsion (wt%)	Dosage of crosslinker (wt%)	Flowback fluid of S-XX-17		Produced water of Z-2#	
			Crosslinking time (s)	Crosslinking performance	Crosslinking time (s)	Crosslinking performance
HAT	1.0	0.2	10~30	Weak crosslinking and almost no hanging	11~31	Weak crosslinking and almost no hanging
		0.3	11~38	Weak crosslinking and almost no hanging	10~39	Weak crosslinking and almost no hanging
		0.4	12~81	Incomplete crosslinking and weak hanging	12~78	Incomplete crosslinking and weak hanging
		0.5	11~93	Incomplete crosslinking and weak hanging	11~89	Incomplete crosslinking and weak hanging
		0.6	12~33	Weak crosslinking and almost no hanging	11~30	Weak crosslinking and almost no hanging
		0.7	10~35	Weak crosslinking and almost no hanging	11~33	Weak crosslinking and almost no hanging
AAT		0.2	11~95	Incomplete crosslinking and weak hanging	12~90	Incomplete crosslinking and weak hanging
		0.3	13~139	Complete crosslinking and strong hanging	11~135	Complete crosslinking and strong hanging
		0.4	14~152	Complete crosslinking and strong hanging	12~148	Complete crosslinking and strong hanging
		0.5	11~112	Complete crosslinking and moderate hanging	10~106	Complete crosslinking and moderate hanging
		0.6	12~105	Complete crosslinking and moderate hanging	11~115	Complete crosslinking and moderate hanging
		0.7	14~78	Incomplete crosslinking and weak hanging	12~75	Incomplete crosslinking and weak hanging
HAT	1.2	0.2	10~76	Incomplete crosslinking and weak hanging	11~73	Incomplete crosslinking and weak hanging
		0.3	12~92	Complete crosslinking and general hanging	12~93	Complete crosslinking and general hanging
		0.4	11~113	Complete crosslinking and moderate hanging	10~105	Complete crosslinking and moderate hanging
		0.5	11~139	Complete crosslinking and strong hanging	12~136	Complete crosslinking and strong hanging
		0.6	13~114	Complete crosslinking and moderate hanging	11~113	Complete crosslinking and moderate hanging
		0.7	10~89	Incomplete crosslinking and general hanging	11~79	Incomplete crosslinking and general hanging
AAT		0.2	11~95	Complete crosslinking and general hanging	11~94	Complete crosslinking and general hanging
		0.3	12~141	Complete crosslinking and strong hanging	10~131	Complete crosslinking and strong hanging
		0.4	13~148	Complete crosslinking and strong hanging	11~139	Complete crosslinking and strong hanging
		0.5	11~139	Complete crosslinking and strong hanging	10~136	Complete crosslinking and strong hanging
		0.6	11~113	Complete crosslinking and moderate hanging	11~108	Complete crosslinking and moderate hanging
		0.7	12~109	Complete crosslinking and moderate hanging	11~100	Complete crosslinking and moderate hanging
HAT	1.4	0.2	11~72	Incomplete crosslinking and weak hanging	10~76	Incomplete crosslinking and weak hanging
		0.3	12~89	Complete crosslinking and general hanging	13~95	Complete crosslinking and general hanging
		0.4	12~110	Complete crosslinking and moderate hanging	11~109	Complete crosslinking and moderate hanging
		0.5	11~149	Complete crosslinking and strong hanging	12~139	Complete crosslinking and strong hanging
		0.6	12~109	Complete crosslinking and moderate hanging	13~122	Complete crosslinking and moderate hanging
		0.7	13~92	Incomplete crosslinking and general hanging	12~84	Incomplete crosslinking and general hanging
AAT		0.2	12~97	Complete crosslinking and general hanging	10~86	Complete crosslinking and general hanging
		0.3	11~154	Complete crosslinking and strong hanging	11~148	Complete crosslinking and strong hanging
		0.4	12~153	Complete crosslinking and strong hanging	11~156	Complete crosslinking and strong hanging
		0.5	11~149	Complete crosslinking and strong hanging	12~145	Complete crosslinking and strong hanging
		0.6	12~113	Complete crosslinking and moderate hanging	11~112	Complete crosslinking and moderate hanging
		0.7	11~107	Complete crosslinking and moderate hanging	10~106	Complete crosslinking and moderate hanging

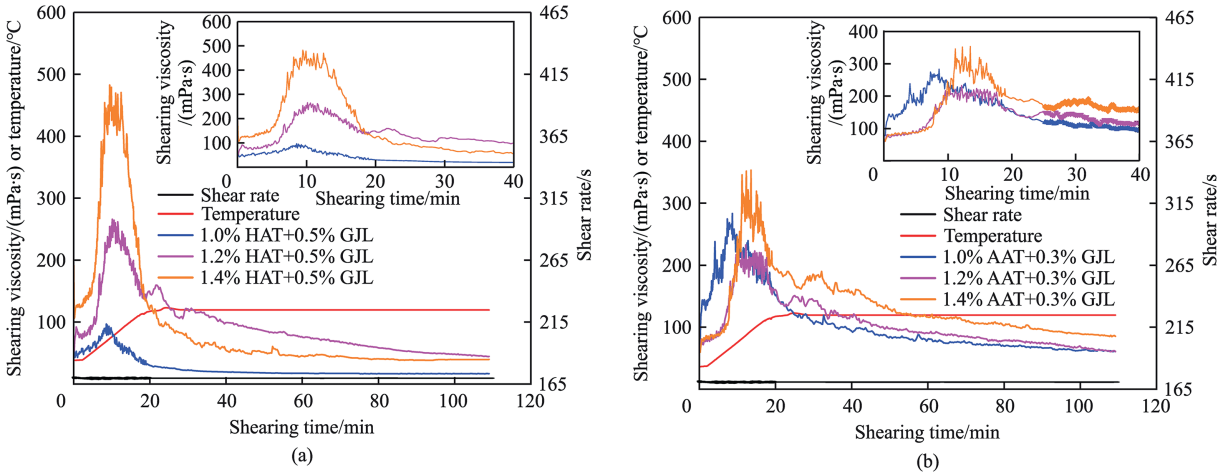

Fig. 16. Variation curves of shearing viscosity of crosslinking system as a function of shearing time in Z-2# produced water: (a) HAT suspended-emulsion + GJL; (b) AAT suspended-emulsion + GJL.

As mentioned above, under the harsh conditions of flowback fluid and produced water, the associative thickener not only has strong crosslinking performance, but also owns the ability of easy to gel-breaking and low damage, which are very benefit to achieve the reutilization of high-salinity flowback fluid and produced water with untreatment in Sulige Gasfield.

3.4.5. Possible interaction mechanism of associative thickener with crosslinker

In fact, many literatures have reported that the common interaction mechanism of synthesized polyacrylamide polymers with organic zirconium crosslinker is mainly that the carboxyl groups ($-COO^-$) on the polymer macromolecular chains can significantly

Table 7
Results of temperature-shear resistance measurement of crosslinking system through online-crosslinking in Z-2# produced water.

Crosslinking system	Initial crosslinking time (min)	Temperature corresponding to initial crosslinking (°C)	Maximum viscosity (mPa·s)	Time corresponding to maximum viscosity (min)	Temperature corresponding to maximum viscosity (°C)	Final stable shearing viscosity (mPa·s)
1.0% HAT+0.5% GJL	3.2	42.3	96.7	8.5	68.8	16.5
1.2% HAT+0.5% GJL	4.3	48.3	265	10.1	82.4	44
1.4% HAT+0.5% GJL	3.4	43.5	478	9.9	85.7	40
1.0% AAT+0.3% GJL	0.2	36.5	283	8.6	69.6	61
1.2% HAT+0.3% GJL	0.2	36.4	232	12.1	86.6	61
1.4% HAT+0.3% GJL	0.2	36.4	353	13.5	93.8	85

Table 8
Static sand-carrying results of different crosslinking systems in flowback fluid and produced water.

Crosslinking system	Flowback fluid of S-XX-17			Produced water of Z-2#		
	Gelation state	Total settling time of proppant (min)	Settling rate of proppant (cm/min)	Gelation state	Total settling time of proppant (min)	Settling rate of proppant (cm/min)
1.2% HAT+0.5% GJL	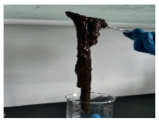	68	0.1324		75	0.1200
1.4% HAT+0.5% GJL	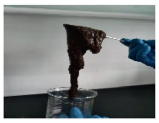	78	0.1154	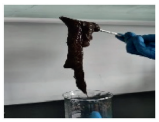	86	0.1047
1.2% AAT+0.3% GJL	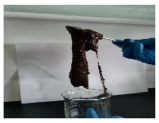	90	0.1000	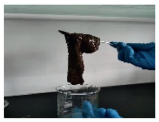	100	0.0900
1.4% AAT+0.3% GJL		115	0.0783	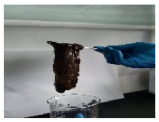	125	0.0720

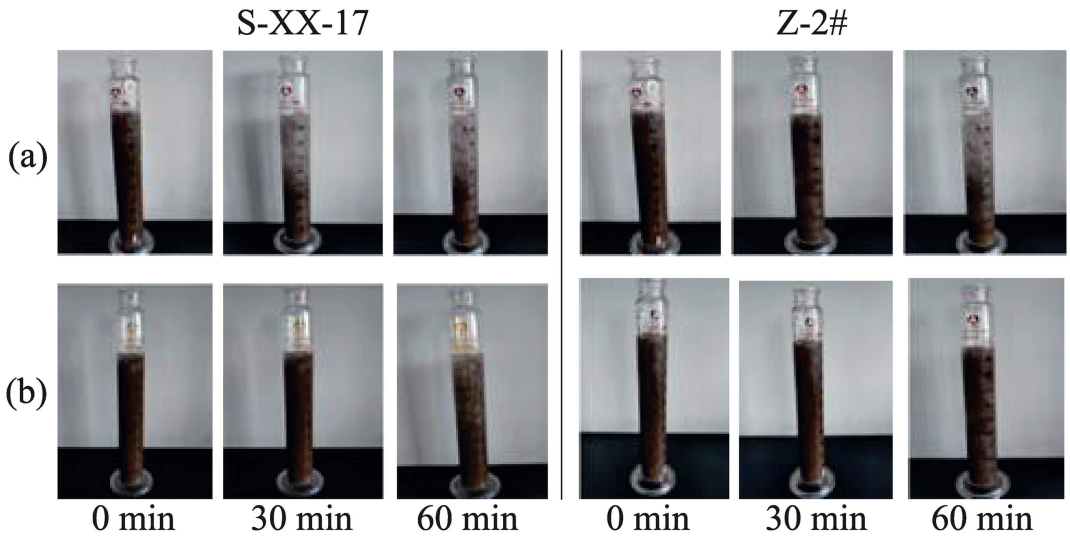

Fig. 17. Images of static sand-carrying measurements of different crosslinking systems in flowback fluid and produced water: (a) 1.2% HAT+0.5% GJL; (b) 1.2% AAT+0.3% GJL.

Table 9
Gel-breaking property of the gel formed by different crosslinking systems at different dosages of gel-breaker after gel-breaking for 90 min.

Crosslinking system	APS (wt%)	Flowback fluid of S-XX-17			Produced water of Z-2#		
		Viscosity (mPa·s)	Surface tension (mN/m)	Residue content (mg/L)	Viscosity (mPa·s)	Surface tension (mN/m)	Residue content (mg/L)
1.2% HAT +0.5% GJL	0.03	6.84	29.02	101	6.13	28.55	89
	0.05	4.68	27.76	60	4.54	27.57	55
	0.07	4.56	27.48	55	4.72	27.16	48
1.2% AAT +0.3% GJL	0.03	7.56	29.44	121	7.26	29.31	111
	0.05	4.45	27.36	58	4.76	27.18	52
	0.07	4.37	27.39	54	4.56	27.44	51

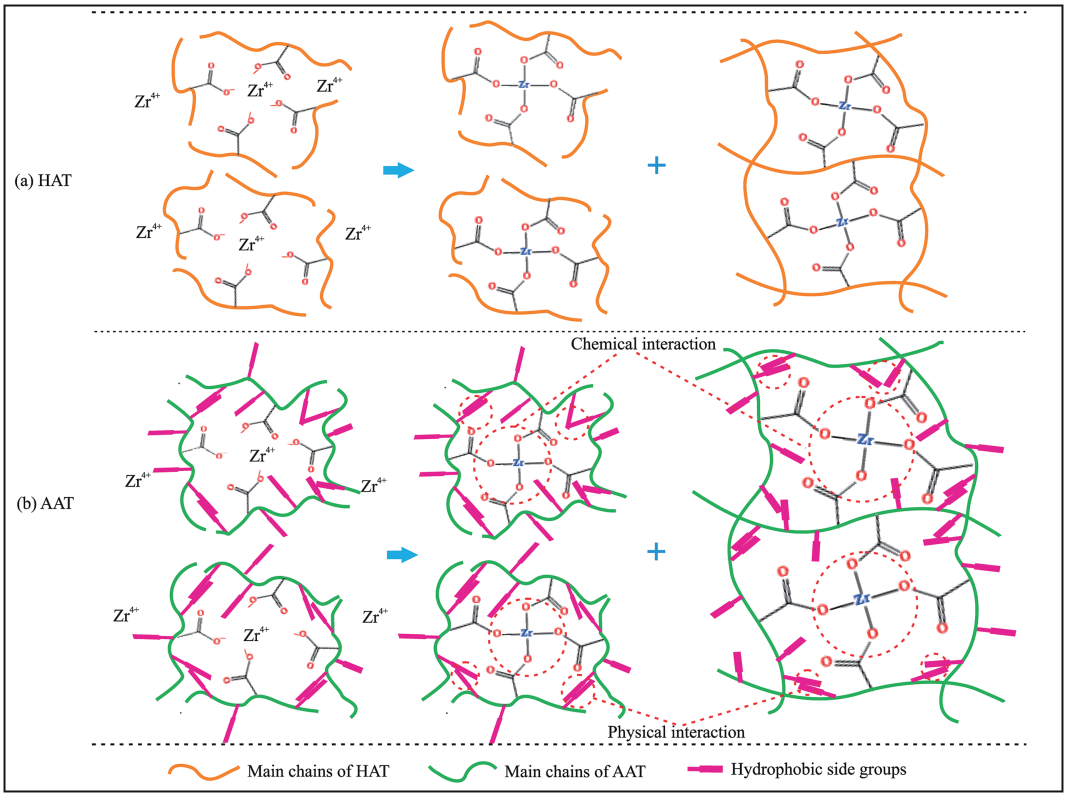

Fig. 18. Possible interaction mechanism of different thickeners with organic zirconium crosslinker.

interact with quadrivalent zirconium ions (Zr^{4+}) released by zirconium crosslinkers to make the macromolecular chains form a strong spatial network structure [23,24,54]. As shown in Fig. 18(a), as a linear polymer, HAT corresponds to the aforementioned mechanism very well. That is, the crosslinking strength of HAT mainly depended on the hydromechanical size of the molecular chain, which directly determines the conformation of final crosslinking network. However, under the conditions of flowback fluid and produced water, the diffusion double-layer of polymer was compressed by metal ions, especially high-valent ions, so that the molecular chains became curly and the hydromechanical size of the molecular chain became smaller noticeably [55]. On the contrary, as for AAT, the diffusion double-layer was also compressed by metal ions, but increasing solution polarity caused by the higher ion content can promote the association effect of hydrophobic side groups, so that the hydromechanical size of the molecular chain and the strength of resulting crosslinking network were relatively greater. In a word, the crosslinking capacity of AAT and resulting gel strength were determined by two aspects of physical and chemical interaction illustrated in Fig. 18(b).

4. Conclusions

In this study, an anti-salt associative thickener (AAT) was synthesized and characterized, and the comprehensive performances of AAT were systematically investigated under different conditions to analyze the feasibility of untreatment reutilization of high-salinity flowback fluid and produced water by using associative thickener. The specific results and findings are as follows:

(1) The FT-IR and ^{1}H-NMR results indicate that the associative thickener can be successfully prepared by the free radical copolymerization of AM, NaAA, AMPS with a small amount of C16MDAC.
(2) Compared with linear thickener, associative thickener can present good comprehensive performances under the harsh conditions of flowback fluid and produced water in Sulige Gasfield, including excellent thickening capacity, good temperature and shear resistance, high drag reduction efficiency, strong sand-carrying ability, easy to gel-breaking and so forth, which implicates the potential and feasibility to

reutilize high-salinity flowback fluid and produced water without further treatment. Moreover, achieving high drag reduction and strong sand-carrying of associative thickener might be ascribed to the existence of reversible supramolecular structures and the significant increase of viscoelasticity by shear stretching in turbulent state.

(3) Associative thickener can achieve the high-effective online-crosslinking with organic zirconium crosslinker at high salinity through the synergistic effect of physical interaction and chemical crosslinking. Specifically, an excellent gelation state, temperature-shear resistance, static sand-carrying capacity and gel-breaking property can be obtained, which are also benefit to achieve the reutilization of high-salinity flowback fluid and produced water with untreatment in Sulige Gasfield.

(4) It has the great potential and feasibility of reutilization of high-salinity flowback fluid and produced water with untreatment by using associative thickener to establishing the fracturing fluid, which can provide an important guidance for the design of novel fracturing fluid and the reutilization of high-salinity water in stimulation applications.

CRediT authorship contribution statement

Yan Liang: Writing – review & editing, Writing – original draft, Visualization, Validation, Project administration, Methodology, Investigation, Funding acquisition, Formal analysis, Data curation, Conceptualization. **Sukai Wang:** Visualization, Validation, Methodology, Investigation, Data curation, Conceptualization. **Guiyi Zhang:** Visualization, Validation, Methodology, Investigation, Conceptualization. **Yonglong Li:** Visualization, Validation, Project administration, Methodology, Data curation. **Wei Liu:** Writing – original draft, Visualization, Validation, Supervision, Methodology. **Songlin Pu:** Writing – original draft, Visualization, Methodology, Investigation. **Lipeng Zhang:** Writing – original draft, Visualization, Methodology, Investigation. **Tianxiang Wang:** Writing – review & editing, Writing – original draft, Visualization, Methodology. **Lianghui Wan:** Writing – review & editing, Writing – original draft, Visualization, Methodology. **Xionghui Liu:** Writing – review & editing, Writing – original draft, Visualization, Methodology.

Declaration of competing interest

The authors declare that they have no known competing financial interests or personal relationships that could have appeared to influence the work reported in this paper.

Acknowledgements

This work was supported financially by the Introduction Program of Tianchi Talent on Young Doctor in Xinjiang (grant No. 2023TCXZGCY01) and the Science and Technology Project of CNPC Western Drilling Engineering Co., LTD (grant No. 2023XZ201). The authors are grateful for the financial support.

References

[1] C.Y. Zhou, M.Y. Lei, M. Zhou, L.H. Zeng, Y. Sun, Q. Huang, Y. Xiao, P. Zhang, Preparation and properties of bifunctional associative polymer with twin tail and long chain structure for shale gas fracturing, Polym. Adv. Technol. 33 (2022) 1069–1078.

[2] L. He, S. Wang, J. Guo, Z. Zhang, Y. Zhang, Research progress of high salinity water-based fracturing fluid technology, Oilfield Chem. 32 (2015) 621–627 (in Chinese).

[3] Q. Lei, B. Guan, B. Cai, X. Wang, Y. Xu, Z. Tong, H. Wang, H. Fu, Z. Liu, Z. Wang, Technological progress and prospects of reservoir stimulation, Petrol. Explor. Dev. 46 (2019) 605–613.

[4] A. Zhang, Z. Yang, X. Li, D. Xia, Y. Zhang, Y. Luo, Y. He, T. Chen, X. Zhao, An evaluation method of volume fracturing effects for vertical wells in low permeability reservoirs, Petrol. Explor. Dev. 47 (2020) 441–448.

[5] T. Xu, J. Mao, Q. Zhang, C. Lin, X. Yang, Y. Zhang, A. Du, M. Cun, Z. Huang, Q. Wang, Synergistic polymer fracturing fluid for coal seam fracturing, Colloids Surf. A Physicochem. Eng. Asp. 631 (2021) 127648.

[6] G. Zou, B. Pan, W. Zhu, Y. Liu, S. Ma, M. Liu, Investigation of fracturing fluid flowback in hydraulically fractured formations based on microscopic visualization experiments, Polymers 15 (2023) 1560.

[7] Q. Lei, D. Weng, S. Xiong, H. Liu, B. Guan, Q. Deng, X. Yan, H. Liang, Z. Ma, Progress and development directions of shale oil reservoir stimulation technology of China National Petroleum Corporation, Petrol. Explor. Dev. 48 (2021) 1198–1207.

[8] H. Shi, X. He, C. Zhou, L. Wang, Y. Xiao, Hydrochemistry, sources and management of fracturing flowback fluid in tight sandstone Gasfield in Sulige Gasfield (China), Arch. Environ. Contam. Toxicol. 84 (2023) 284–298.

[9] S. Yu, C. Chang, X. Chen, Differential treatment and reuse technology of fracturing flow-back fluid in Sulige gas field, Ind. water Treat. 43 (2023) 195–200.

[10] J. Fajfer, O. Lipińska, M. Konieczyńska, Hydraulic fracturing flowback chemical composition diversity as a factor determining possibilities of its management, Environ. Sci. Pollut. Control Ser. 29 (2022) 16152–16175.

[11] J. Shao, L. You, Y. Kang, M. Chen, J. Tian, Salinity of flowback fracturing fluid in shale reservoir and its reservoir damage: experimental and field study, J. Petrol. Sci. Eng. 211 (2022) 110217.

[12] S. Chen, F. Hui, W. Wei, K. Li, J. Wei, M. Pang, Z. Liang, Experimental study and application of clean fracturing fluid flowback fluid flooding in tight sandstone reservoir, Drill. Prod. Technol. 43 (2020) 100–103 (in Chinese).

[13] X. Zhang, Research and application of high-efficiency bactericide for recycling of fracturing flowback fluid, Drill. Prod. Technol. 40 (2017) 112–114 (in Chinese).

[14] X. Chen, Y. Lu, Y. Wu, L. Ma, Analysis of policy and enlightenment on treatment of fracturing fluid in shale gas production between China and the United States, J. Southwest Petrol. Univ. (Sci. Tech. Ed.) 43 (2021) 212–219 (in Chinese).

[15] Y. Zhang, J. Mao, J. Mao, A. Chen, X. Yang, C. Lin, Z. Wei, X. Huang, L. Song, F. Tang, Q. Jiang, Y. Ni, Towards sustainable oil/gas fracking by reusing its process water: a review on fundamentals, challenges, and opportunities, J. Petrol. Sci. Eng. 213 (2022) 110422.

[16] B. Yang, J. Zhao, J. Mao, H. Tan, Y. Zhang, Z. Song, Review of friction reducers used in slickwater fracturing fluids for shale gas reservoirs, J. Nat. Gas Sci. Eng. 62 (2019) 302–313.

[17] Y. Zhang, J. Mao, J. Zhao, X. Yang, Z. Zhang, B. Yang, W. Zhang, H. Zhang, Preparation of a novel ultra-high temperature low-damage fracturing fluid system using dynamic crosslinking strategy, Chem. Eng. J. 354 (2018) 913–921.

[18] R. Barati, J.-T. Liang, A review of fracturing fluid systems used for hydraulic fracturing of oil and gas wells, J. Appl. Polym. Sci. 131 (2014).

[19] Y. Fan, W. Yu, W. Shu, Y. Zhang, Y. Ju, P. Fan, Synthesis and performance evaluation of low-damage variable viscosity integrated drag reducer, J. Appl. Polym. Sci. 141 (2024) e55925.

[20] C. Zuo, Y. Wu, K. Du, L. Zhu, Z. Gou, Y. Xia, Z. Jia, W. Zeng, Preparation and laboratory study of a sodium carboxymethyl cellulose smart temperature-controlled crosslinked gel fracturing fluid system, J. Appl. Polym. Sci. 140 (2023) e54380.

[21] S. Shi, J. Sun, K. Lv, Q. Wen, Y. Bai, J. Wang, J. Jin, J. Liu, X. Huang, J. Li, Preparation and evaluation of acryloyl morpholine modified emulsion fracturing fluid thickener with high temperature resistance and salt resistance, J. Appl. Polym. Sci. 140 (2023) e53338.

[22] C. Dai, Y. Huang, C. Liu, Y. Wu, C. Zou, X. Yan, Q. Liu, M. Cao, Progress and prospect of fracturing fluid system for deep/ultra-deep reservoir reconstruction, J. Chin. Univ. Petrol. (Ed. Nat. Sci) 47 (2023) 78–92 (in Chinese).

[23] M. Zhou, J. Zhang, Z. Zuo, M. Liao, P. Peng'ao, Preparation and property evaluation of a temperature-resistant Zr-crosslinked fracturing fluid, J. Ind. Eng. Chem. 96 (2021) 121–129.

[24] H. Xin, B. Fang, L. Yu, Y. Lu, K. Xu, K. Li, Rheological performance of high-temperature-resistant, salt-resistant fracturing fluid gel based on organic-zirconium-crosslinked HPAM, Gels 9 (2023) 151.

[25] E. Yao, H. Xu, Y. Li, X. Ren, H. Bai, F. Zhou, Reusing flowback and produced water with different salinity to prepare guar fracturing fluid, Energies 15 (2022) 153.

[26] F. Xiong, X.-Q. Wang, Y. Liu, L. Chen, Z.-H. Zhao, H. Yang, J.-Y. Hu, D. Li, Y. Zhang, Y.-D. Li, Experimental study on the effect of tight gas fracturing flowback fluid composition on the performance of modified polyacrylamide viscosity reducing and slippery water system, J. Appl. Polym. Sci. 140 (2023) e54281.

[27] S. Kim, P. Omur-Ozbek, A. Dhanasekar, A. Prior, K. Carlson, Temporal analysis of flowback and produced water composition from shale oil and gas operations: impact of frac fluid characteristics, J. Petrol. Sci. Eng. 147 (2016) 202–210.

[28] Z. Wang, Z. Lv, J. Dong, F. Zhang, P. Zhou, Influence of multivalent metal ions on organic borate-crosslinked guanidine gum fracturing gluids: analysis and

countermeasures, J. Southwest Petrol. Univ. (Sci. Tech. Ed.) 41 (2019) 177–184 (in Chinese).
[29] E. Mohammad-Pajooh, D. Weichgrebe, G. Cuff, B.M. Tosarkani, K.-H. Rosenwinkel, On-site treatment of flowback and produced water from shale gas hydraulic fracturing: a review and economic evaluation, Chemosphere 212 (2018) 898–914.
[30] B. Yang, H. Zhang, Y. Kang, L. You, J. She, K. Wang, Z. Chen, In situ sequestration of a hydraulic fracturing fluid in Longmaxi shale gas formation in the Sichuan Basin, Energy & Fuels 33 (2019) 6983–6994.
[31] J. Jing, G. Qu, H. Wei, J. Yan, X. Chen, W. Yu, S. Li, Recycle technology of fracturing flowback fluid in Sulige Gasfield, Xinjiang Oil Gas 17 (2021) 36–40 (in Chinese).
[32] T. Zhao, Treatment technology of shale gas fracturing flowback fluid: a mini review, Front. Energy Res. 11 (2023).
[33] Y. Zhang, J. Mao, J. Mao, A. Chen, X. Yang, C. Lin, Z. Wei, X. Huang, L. Song, F. Tang, Q. Jiang, Y. Ni, Towards sustainable oil/gas fracking by reusing its process water: a review on fundamentals, challenges, and opportunities, J. Petrol. Sci. Eng. 213 (2022) 110422.
[34] Q. Zhang, J. Mao, X. Yang, C. Lin, H. Zhang, T. Xu, Q. Wang, Synthesis of a hydrophobic association polymer with an inner salt structure for fracture fluid with ultra-high-salinity water, Colloids Surf. A Physicochem. Eng. Asp. 636 (2022) 128062.
[35] X. Liang, M. Wu, Y. Yang, D. Liu, X. Li, Shale gas hydraulic fracturing flowback fluid treatment using a modified vortex flocculation reactor: effects of the axial and tangential inlet angles, Chem. Eng. Sci. 275 (2023) 118713.
[36] Q. He, C. Yin, J. Li, Z. Pu, Y. Li, J. Zhang, Research and application on reuse technology of shale gas fracturing flowback fluid in Weiyuan-Changning area, Drill. Prod. Technol. 39 (2016) 118–121 (in Chinese).
[37] H. Fan, H. Yang, L. Li, Z. Wei, S. Zhang, J. Zhang, S. Liu, h. Yang, Cross-linking and temperature resistance property of alcohol-containing fracturing fluid, J. Chin. Univ. Petrol. (Ed. Nat. Sci) 45 (2021) 120–126 (in Chinese).
[38] T. Liang, L. Shao, E. Yao, J. Zuo, X. Liu, B. Zhang, F. Zhou, Study on fluid-rock interaction and reuse of flowback fluid for gel fracturing in desert area, Geofluids 2018 (2018) 8948961.
[39] P. Coomarasamy, D.F. Mohshim, A.H. Basri, R. Nasir, H. Mukhtar, Performance evaluation of reusing produced water as fracking fluid in Angsi field, Chem. Pap. 76 (2022) 1567–1578.
[40] C. Ke, L. Peng, X. Li, W. Sun, Y. Wei, L. Zhang, Q. Zhang, X. Zhang, Study on reuse of fracturing flowback fluids in Sulige Gasfield, Oilfield Chem. 37 (2020) 409–414 (in Chinese).
[41] J. Mao, C. Li, H. Jiang, H. Zhang, X. Yang, C. Lin, Y. Zhang, D. Wang, Y. Zhang, Y. Song, Preparation of a novel polymer suspensions with high stabilization, and their superior performances in high salinity, J. Mol. Struct. 1297 (2024) 136922.
[42] L. Luo, Y. Wang, G. Qu, Y.H. Yang, F. Jia, Development and application of integrated multi-function anti-salt thickener, Drill. Fluid Complet. Fluid 39 (2022) 383–389 (in Chinese).
[43] Y. Liang, Z. Song, S. Pu, S. Wang, G. Zhang, L. Wan, S. Han, H. Wang, Effect of chemical additives on the stability and performance of suspended-emulsion fracturing fluid formed by associative thickener, J. Polym. Res. 31 (2024) 115.
[44] Y. Liang, Z.-l. Wang, Y.-x. Jin, Y.-q. Tian, X.-m. Liu, Y.-j. Guo, L. Fan, J. Wang, X.-m. Zhang, M. Cao, M.-y. Zhou, Heterogeneity control ability in porous media: associative polymer versus HPAM, J. Petrol. Sci. Eng. 183 (2019) 106425.
[45] V. González Coronel, E. Jiménez-Regalado, Rheological properties of three different microstructures of water-soluble polymers prepared by solution polymerization, Polym. Bull. 67 (2011) 251–262.
[46] Y. Liang, Y. Guo, X. Yang, R. Feng, X. Zhang, H. Li, Insights on the interaction between sodium dodecyl sulfate and partially hydrolyzed microblock hydrophobically associating polyacrylamides in different polymer concentration regimes, Colloids Surf. A Physicochem. Eng. Asp. 572 (2019) 152–166.
[47] L.L. Wang, Y. Liang, W.H. Li, G.W. Yuan, M. Cao, Effect of ion composition on the salt-tolerance behavior of medium-low molecular weight polymers, J. Southwest Petrol. Univ. (Sci. Tech. Ed.) 45 (2023) 174–184 (in Chinese).
[48] P. Kujawa, A. Audibert-Hayet, J. Selb, F. Candau, Effect of ionic strength on the rheological properties of multisticker associative polyelectrolytes, Macromolecules 39 (2006) 384–392.
[49] M. Ding, Y. Han, Y. Liu, Y. Wang, P. Zhao, Y. Yuan, Oil recovery performance of a modified HAPAM with lower hydrophobicity, higher molecular weight: a comparative study with conventional HAPAM, HPAM, J. Indust Eng. Chem. 72 (2019) 298–309.
[50] J. Guo, Y. Li, S. Wang, Adsorption damage and control measures of slick-water fracturing fluid in shale reservoirs, Petrol. Explor. Dev. 45 (2018) 336–342.
[51] H. Tan, J. Mao, W. Zhang, B. Yang, X. Yang, Y. Zhang, C. Lin, J. Feng, H. Zhang, Drag reduction performance and mechanism of hydrophobic polymers in fresh water and brine, Polymers 12 (2020) 955–972.
[52] J. Bao, Fundamental Research of Hydrophobicallyassociating Water-Soluble Polymer Fracturing Liquid Used in Shale Gas Reservoir Stimulated Reservoir Volume Fracturing, Southwest Petroleum University, 2015. Thesis.
[53] N. Le Brun, I. Zadrazil, L. Norman, A. Bismarck, C.N. Markides, On the drag reduction effect and shear stability of improved acrylamide copolymers for enhanced hydraulic fracturing, Chem. Eng. Sci. 146 (2016) 135–143.
[54] G. Miao, H. Zhang, Y. Yang, J. Qu, X. Ma, J. Zheng, X. Liu, Synthesis and performance evaluation of crosslinker for seawater-based fracturing fluid, J. Appl. Polym. Sci. 140 (2022) 53372.
[55] C. Du, W. Wang, Z. Wang, X. Lu, Mechanism of cation on viscosity loss of polyacrylamide solution, J. Chin. Univ. Petrol. (Ed. Nat. Sci) 44 (2020) 164–168 (in Chinese).